Atmospheric Environment 344 (2025) 120976

Contents lists available at ScienceDirect

Atmospheric Environment

journal homepage: www.elsevier.com/locate/atmosenv

Measurements and model results of a two-year dataset of ammonia exchange over a coniferous forest in the Netherlands

E.A. Melman [a,b,*], S. Rutledge-Jonker [a], K.F.A. Frumau [c], A. Hensen [c], W.A.J. van Pul [a], A.P. Stolk [a], R.J. Wichink Kruit [a], M.C. van Zanten [a,b]

[a] National Institute for Public Health and the Environment (RIVM), P.O. Box 1, 3720 BA, Bilthoven, The Netherlands
[b] Meteorology & Air Quality group (MAQ), Wageningen University & Research (WUR), P.O. Box 47, 6700 AA, Wageningen, The Netherlands
[c] Netherlands Organisation for Applied Scientific Research (TNO), P.O. Box 15, 1755 ZG, Petten, The Netherlands

HIGHLIGHTS

- NH_3 exchange was measured over a temperate douglas fir forest in the Netherlands.
- Fluxes were inferred with the gradient method, incl. a roughness sublayer correction.
- Measured fluxes were compared to output of an inferential model (DEPAC).
- Adding a temperature correction in the external leaf path improved model performance.
- Over the past decades concentration has stayed constant and deposition decreased.

ARTICLE INFO

Keywords:
NH_3 exchange
Forest
Measurements
DEPAC
Aerodynamic gradient method
Roughness sublayer

ABSTRACT

In this study we present and analyse a two-year dataset of NH_3 exchange over a temperate Douglas fir forest in the Netherlands. The atmospheric NH_3 concentration ($[NH_3]$) was measured at multiple heights above the canopy in 2009 and 2010. We applied the aerodynamic gradient method combined with four different methods for roughness sublayer correction to calculate fluxes. The results with and without this correction were on average similar, but instantaneous differences can be up to 30%. We evaluated a 1-D inferential model (DEPAC). The reference run tended to overestimate deposition and did not predict emission. The observed stomatal emission potential (Γ_s) agrees well with values from literature and the modelled relation in DEPAC. The model performance strongly improved after implementation of a temperature dependent scaling factor in the external leaf pathway. We estimated the annual deposition load by combining observed and modelled fluxes and subsequent extrapolation of the mean (median) flux to be 11.8 ± 3.5 (8.5 ± 2.6) kg N ha^{-1} in 2009 and 11.4 ± 3.4 (8.7 ± 2.6) kg N ha^{-1} in 2010. Compared to historical measurements in the nineties at the same site, the $[NH_3]$ has stayed approximately constant and the deposition has decreased. Further research has to be done to better quantify these trends and to assess how the newly proposed external leaf pathway in DEPAC behaves in large scale transport models.

1. Introduction

Long-term high-resolution measurements of ammonia (NH_3) exchange between forests and atmosphere are scarce and may reveal different diurnal patterns on seasonal scales. Although exchange of NH_3 is relatively well studied on grass ecosystems, practical challenges have prevented extensive studies on forest ecosystems and such long term datasets are scarce (Guo et al., 2022). A multi-year dataset, however, allows us to investigate the exchange processes in different phenological and meteorological conditions as highlighted by diurnal and seasonal patterns. In this study we present a two-year dataset of NH_3 exchange between forest and atmosphere and analyse it on different temporal scales.

* Corresponding author at: National Institute for Public Health and the Environment (RIVM), P.O. Box 1, 3720 BA, Bilthoven, The Netherlands.
E-mail address: ewout.melman@rivm.nl (E.A. Melman).

https://doi.org/10.1016/j.atmosenv.2024.120976
Received 28 June 2024; Received in revised form 28 October 2024; Accepted 4 December 2024
Available online 31 December 2024

Dry deposition of NH_3 on natural ecosystems has been a topic of interest for a long time and there is common consensus that excess availability of NH_3 causes soil acidification and eutrophication, leading to decreased biodiversity (Clark et al., 2013; Bleeker et al., 2011). In the Netherlands this is a particular pressing issue due to the high input of reactive nitrogen on nature areas by agricultural and industrial activity (de Vries et al., 2021) and various measurement activities are undertaken to monitor. A National Air Quality Monitoring Network (LML) was installed with 8 locations in 1992, measuring hourly concentrations of various atmospheric compounds including NH_3 (van Elzakker et al., 1995). A second network to measure monthly NH_3 concentrations was installed in 2006 and nowadays contains over 300 concentration measurement locations (MAN-network) (Wichink Kruit et al., 2021). Finally, there are currently 4 sites where monthly NH_3-deposition is being measured (Wichink Kruit et al., 2021). Although forest ecosystems are not part of these programs, a series of dry deposition measurement campaigns have been carried out at a forest site (Speulderbos, NL) over the past decades. The first measurement series was part of the Additional Research program Acidification (APV) and carried out between April 1988 and March 1990 (Duyzer et al., 1992). From November 1992 until December 1995 and from July 1996 until November 1998 measurements were continued within the European LIFE and LIFE II framework (Mennen et al., 1997; Erisman et al., 1998; Vonk et al., 2000). Additionally, dry deposition of NH_x ($NH_3 + NH_4^+$) was estimated from throughfall measurements between 1995 and 2000 by Erisman et al. (2001b) and annually updated until 2010 (see Table A.1). Although at the time these measurements were state of the art, these datasets have considerable uncertainties and in general a low temporal coverage. More recently the attention shifted from acidification to eutrophication. In that context, measurements were carried out again from September 2008 to December 2010 as part of the NitroEurope (NEU) framework (Owen et al., 2011). These measurements were done with, at that time, state of the art technology (GRAHAM, Wichink Kruit et al., 2007) and such provide a valuable dataset.

Exchange of NH_3 above forests has been primarily studied with the aerodynamic gradient method (AGM) (Duyzer et al., 1992; Wyers et al., 1992, 1993; Sutton et al., 1993; Duyzer et al., 1994; Mennen et al., 1997; Erisman et al., 1998; Wyers and Erisman, 1998; Andersen et al., 1999; Vonk et al., 2000; Pryor et al., 2001; Neirynck et al., 2005; Hayashi et al., 2011; Xu et al., 2023; Walker et al., 2023). The use of AGM above forests, however, comes with extra challenges as the rough surface disturbes the turbulence, making the classic Monin-Obukhov Similarity Theory (MOST) invalid (Thom et al., 1975). The affected layer is referred to as the roughness sublayer (RSL) and separates itself from the inertial sublayer (ISL, where MOST is valid), which together form the atmospheric surface layer (ASL). The RSL is estimated to reach 1.5–2.5 times the canopy height (Arya, 2001), and thus often logistical issues prevent from measuring above the RSL. Several studies have worked on extensions of MOST to account for the enhanced turbulence (e.g. Bosveld, 1997; Harman and Finnigan, 2007, 2008; De Ridder, 2010). To overcome the invalidity of MOST altogether, advancements have been made with NH_3 measurement techniques that are not affected by the RSL: With the relaxed eddy accumulation (REA) technique (Hansen et al., 2013, 2015) and with the Eddy Correlation (EC) method (Guo et al., 2022).

Previous studies found that NH_3 exchange is influenced by meteorology, chemistry, canopy and leaf structure, chemical and physical characteristics of the surface, organic matter decomposition, soil microbial turnover (Andersen et al., 1999; Flechard et al., 2013), and in particular the surface wetness (Wyers and Erisman, 1998; Hansen et al., 2015). Exchange of NH_3 can take place through the stomata, external leaf surface and soil. During daytime, the plant stomata are open and NH_3 exchange can take place through all pathways, while at night, stomata are closed and exchange only occurs through the soil and external leaf surface pathways.

The size and direction of the flux through these pathways is influenced by compensation points. A compensation point (χ_c) is defined as the atmospheric concentration where the NH_3 flux is zero (Flechard et al., 2013). Farquhar et al. (1980) were the first to demonstrate a compensation point for NH_3 for beans. Later, a compensation point of 1–2 μg m^{-3} was found by Duyzer et al. (1994) for Douglas fir trees at Speulderbos, although the authors indicate that determining a compensation point for a forest may be more complicated and the history of the surface exposure to NH_3 should be taken into account. Most recent models use the canopy compensation point, split up into separate compensation points for the various pathways (which are relevant during different times of the day), to estimate fluxes (Neirynck and Ceulemans, 2008; Massad et al., 2010; Zhang et al., 2010; van Zanten et al., 2010). In the Netherlands the flux is calculated with the DEPAC-1D module (as part of large scale transport models) (van Zanten et al., 2010), which incorporates compensation points for the stomatal and external leaf pathways.

Even though a number of studies into forest-atmosphere NH_3 exchange have been performed, often the number of observations is limited or come with large uncertainty. A long dataset with high temporal resolution and coverage during both day and night and over multiple seasons allows us to study exchange processes which are relevant during different environmental conditions. Therefore, in this study, we present and analyse a two-year high resolution dataset of NH_3 exchange between forest and atmosphere.

The main objectives of this study are to (i) show the effect of including the RSL turbulent conditions in flux calculations, (ii) show seasonal and diurnal variability in NH_3 exchange, (iii) show the performance of the one dimensional dry deposition module DEPAC-1D (DEPosition of Acidifying Components) and (iv) identify long term trends in the yearly deposition load by comparing the data presented here with historically obtained data. To this end, we will analyse the half-hourly concentrations measurements at three levels above the canopy, collected at Speulderbos between September 2008 and December 2010. Furthermore, we will evaluate the DEPAC module and use it to estimate the yearly deposition load.

2. Data & methods

2.1. Observation site

NH_3 concentration ($[NH_3]$) and meteorological observations were collected at the 'Speulderbos' forest (52.25° N, 5.69° E) (see e.g. Duyzer et al. (1992) and Schilperoort et al. (2020)). This mixed forest is located in the middle of the Netherlands, in the northwest of nature area 'the Veluwe'. The measurement tower is marked with a red triangle in Fig. 1a and is directly surrounded by a homogeneous Douglas fir patch (DFP). The DFP had a mean canopy height (h_c) of 32 m in 2006, is dense and has no understory. The leaf area index (LAI) was estimated to be 6.1 m^2m^{-2} (Mustafa et al., 2013). The DFP is of limited size. From the tower, the DFP extends 45 m to the north, 80 m to the east, 50 m to the south and 160 m to the west. The DFP is surrounded with other patches with species like Beech or Scots Pine. A flux footprint analysis (Kljun et al., 2015) showed that at least 70% of the flux originates from the DFP. More information on the influence of the limited fetch can be found in Supplementary material S2 of Melman et al. (2024a). Beyond the DFP, the shortest distance to the forest edge is ~900 m in the southeast direction. On a larger scale, there is agricultural activity (including stables) towards the southwest and to a lesser extend towards the south/southeast. The forest stretches the furthest towards the north.

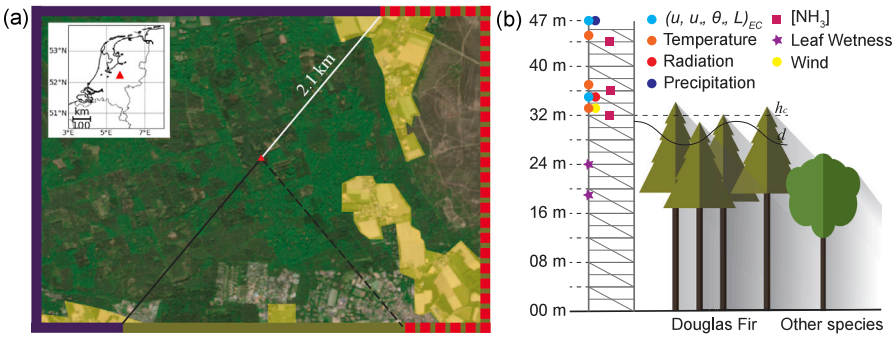

Fig. 1. (a) Observation site. Satellite images were retrieved from dataspace.copernicus.eu and the length of the white line indicates the scale (2.1 km). The coloured outline indicates the disturbed sector (red dashed), high concentration sector (green) and low concentration sector (purple), as defined in Section 3.2. The yellow shaded markings indicate agricultural fields, based on land use maps from 2007/2008 (LGN6, www.lgn.nl). Note that these markings correspond to agricultural fields and do not necessarily correspond to emission areas during the measurement campaign. (b) Overview of the measurement tower.

2.2. Data collection & treatment

NH_3 concentration was measured with a GRadient Ammonia High Accuracy Monitor (GRAHAM) from a 46 m tall tower at three levels (32 m, 36 m and 44 m) between 01-09-2008 and 31-12-2010. The GRAHAM is an advanced version of the AMANDA instrument (Wyers et al., 1993; Wyers and Erisman, 1998) and has an higher precision (Wichink Kruit et al., 2007). The GRAHAM measures the NH_3 concentration with an annular denuder system, connected to a detector unit. Detailed descriptions of the GRAHAM equipment and the measurement technique are given in Wichink Kruit et al. (2007) and Wichink Kruit (2010). The GRAHAM has a level of detection (LoD) of 0.1 μg m^{-3} and a precision of 1.9% and measures at 10 min intervals, which we averaged to 30 min values. The systematic error of the GRAHAM was determined to be 0.6% by Wichink Kruit (2010).

In 2008, data coverage was very low and therefore discarded. In 2010 the concentration measurements from the middle level did not pass technical validation. In hindsight, we observed similar deviating patterns in 2009; therefore, we removed the middle level from further analysis in order to assure a consistent dataset. A sensitivity study on ignoring the middle level when doing flux calculations for the same instrument located in a dune area was done by Vendel et al. (2023). They found that using only the lowest and highest levels instead of all three levels had a negligible (0.1%) impact on the flux. From the end of November 2009 to the end of March 2010 the GRAHAM was turned off to protect it from freezing. This resulted in a large data gap of almost 4 months. Most other gaps in the time series are less than 1 day, but several gaps of 7 + days exist, which arose due to technical issues.

Next to [NH_3], standard meteorological parameters such as temperature, turbulent variables, wind velocity, precipitation, radiation and leaf wetness were collected as part of the NitroEurope (NEU) project (Owen et al., 2011). Temperature was measured at 33, 37 and 45 m (thermocouples type E, TC inc., USA). Turbulent variables (including the Obukhov length (L), wind speed and wind direction) were measured with two 3D 20 Hz sonic anemometers (CSAT3, Campbell Sci. Inc., USA) installed at 35 m and 47 m and subsequently processed using Alteddy software (Elbers, 1998). Wind velocity was measured at an additional level at 33 m with a Mierij MMW05 sensor (MMW05, Mierij Meteo, NL) until mid-June 2009 and afterwards with a Gill 2D sensor (Gill sonic 2D, Gill instruments Ltd, UK). Precipitation was measured at 47 m (WXT510, Vaisala, FIN) and radiation data was collected at 47 m (CNR1, Kipp & Zonen BV, NL). Finally, leaf wetness was measured at 19 m and at 24 m (237 grid, Campbell Sci. Inc., USA). An overview of the locations of the instruments is given in Fig. 1b.

To assure high quality data, we filtered the NH_3 concentration data with filters 1 and 2 and NH_3 fluxes with filters 1–6 from Table 1. Filter 1 excludes measurements where data did not pass technical validation to assure high quality data. Filter 2 identifies whether the data makes physically sense (i.e. with no negative concentrations at $z = z_0$) and the measured concentration at the reference height (z = 1m) is above the level of detection (LoD) of the GRAHAM. Filter 3 was introduced to exclude disturbance created by the measurement set up. We used the quality flags from EC output to assure stationarity with Filter 4, which is an important assumption for the AGM. Filter 5 was introduced to select moments with a coupled forest-atmosphere only, with the threshold of 0.4 m s^{-1} as derived for the Speulderbos by Schilperoort et al. (2020). Under extremely unstable conditions Eq. (1) does not converge and will lead to inaccurate results. Therefore, these points are filtered out (filter 6) based on the estimate of the displacement height (Melman et al., 2024a).

2.3. Flux calculation

The exchange of NH_3 was determined with the aerodynamic gradient method (AGM). Due to the tall canopy and the limited tower height the gradient was measured inside the roughness sublayer (RSL). In a previous study (Melman et al., 2024a), we evaluated two methods to account for the RSL: The α-factor (which has been applied on NH_3 fluxes at this site before) (Bosveld, 1997; Duyzer et al., 1992) and the method of Harman and Finnigan (2007, 2008) (hereafter HF07/08). In brief, the α-factor is an observational based method that scales MOST, while the HF07/08 method is a physically based extension of MOST. Each of the methods was able to reproduce the sensible heat flux as measured by the EC (H_{EC}) and has different practical advantages. We expected that the choice of the approach used to extent MOST for RSL effects would be the largest contributing factor to the uncertainty in the flux, hence we use both methods as an ensemble to investigate their spread. For completeness, we also calculate the flux with MOST:

$$F_{NH_3} = -\kappa u_* \frac{\chi(z_2) - \chi(z_1)}{ln\left(\frac{z_2-d}{z_1-d}\right) - \Psi_H(\zeta_2) + \Psi_H(\zeta_1)} \quad (1)$$

where χ denotes NH_3 concentration, κ is the von Kàrmàn constant (0.4), u_* the friction velocity, z the measurement height, $\Psi_H(\zeta)$ the integrated form of $\phi_H(\zeta)$ and ζ the atmospheric stability ($(z-d)L^{-1}$). In this study, we use the functions by Paulson (1970) and Dyer (1974) for unstable situations (i.e. $\zeta < 0$) and the functions by Beljaars and Holtslag (1991) for stable situations (i.e. $\zeta \geq 0$). We assume that the flux-profile relations for heat and NH_3 are equal (i.e. $\phi_H = \phi_\chi$). d denotes the displacement height for which we use the relation with the mean canopy height (h_c) from Weligepolage et al. (2012), which gives d = 27 m. When using the α-factor the flux is calculated as:

$$\zeta < 0: \quad F_{NH_3} = -\kappa u_* \frac{\chi(z_2) - \chi(z_1)}{\alpha_H\left(ln\left(\frac{z_2-d}{z_1-d}\right) - \Psi_H(\zeta_2) + \Psi_H(\zeta_1)\right)} \quad (2)$$

$$\zeta \geq 0: \quad F_{NH_3} = -\kappa u_* \frac{\chi(z_2) - \chi(z_1)}{\alpha_H ln\left(\frac{z_2-d}{z_1-d}\right) - \Psi_H(\zeta_2) + \Psi_H(\zeta_1)} \quad (3)$$

Table 1
Filter criteria for NH_3 flux measurements. Data was collected between 01-01-2009 and 31-12-2010. Acceptance rate shown applies to filter criteria applied in sequence.

Filter #		Condition	Acceptance	
			2009	2010
	Measurement period		100%	100%
0	Successful sampling		51.9%	43.8%
1	Instrumental quality check		45.0%	43.3%
2	Data quality check	$[NH_3](z = z_0) > 0$	41.8%	31.4%
		$[NH_3](z_{ref}) > LoD$	41.7%	31.2%
3	Undisturbed region[a]	WD ≤ 40 or WD ≥ 160	30.8%	23.0%
4	Stationarity[a b]	QF $H_{EC} \leq 3$	27.4%	20.2%
5	Coupled forest-atmosphere[a]	$u_* > 0.4$	15.6%	11.4%
6	Physical d[a c]	$d_{HF} > 25$ m	15.5%	11.4%

[a] For flux only.
[b] Based on Foken et al. (2006).
[c] See Section 4 of Melman et al. (2024a).

We derived the α-factor as described in Melman et al. (2024a), but removed Filter 11 ($H \leq Q_{net}$) from their Table 1. This filter created a bias during nighttime and removal improved the results (i.e. resulted in a better agreement between AGM and EC flux) of the α-factor with 4%. In this study, we used two submethods: a constant α-factor (MOST + $\alpha_{constant}$, with $\alpha_M = 0.92$ for the momentum flux and $\alpha_H = 0.84$ for the NH_3 flux) and a directional dependent α-factor (MOST + $\alpha_{directional}$, varying between 0.73 and 0.94 with bins of 20°).

When using the HF07/08 method the flux is calculated as:

$$F_\chi = -\kappa u_* \frac{\chi(z_2) - \chi(z_1)}{ln\left(\frac{z_2-d}{z_1-d}\right) - \Psi_H(\zeta_2) + \Psi_H(\zeta_1) + \hat{\Psi}_H(\zeta_2, \delta_w) - \hat{\Psi}_H(\zeta_1, \delta_w)} \tag{4}$$

where δ_w denotes the vorticity thickness. HF07/08 introduce their own method for d, given by:

$$d = h_c - \beta^2 L_c \tag{5}$$

Here, β denotes a stability dependent parameter proportional to the surface drag (c_d) and given by:

$$\beta = u_*/\bar{u}(h_c). \tag{6}$$

L_c denotes the canopy penetration depth, for which we used the for this site optimized value of $L_c = 30$ m (Melman et al., 2024a). With this method a separate d for each 30 min period is calculated. β can also be parameterized as a function of stability and site-specific parameters. We include both the observed β and parameterized β, and, hence, we have two sub-methods for the HF07/08 scheme. For more information on the flux calculation methods described above we refer to Melman et al. (2024a) and the papers of Harman and Finnigan (2007, 2008), Harman (2012) and Duyzer et al. (1992).

We used a linear regression to calculate the stability corrected gradient, following Wichink Kruit et al. (2009) and Vendel et al. (2023). Finally, we determined the flux by taking the average of the RSL corrected fluxes as calculated by the four different methods. This will be referred to as MOST+RSL or observed (in contrast to MOST, which does not account for the RSL and is also incorporated in the analysis).

2.4. Flux error estimate

We identified four sources of (possible) error on the fluxes. First, uncertainties in measured parameters causes random errors in the flux. The absolute random error is given by:

$$\delta F_\chi = |F_\chi| \cdot \sqrt{\left(\frac{\delta u_*}{|u_*|}\right)^2 + \left(\frac{\delta[NH_3]}{\Delta[NH_3]}\right)^2 + \left(\frac{\delta f(z,\Psi)}{f(z,\Psi)}\right)^2} \tag{7}$$

The uncertainties in δu_* and $\delta[NH_3]$ were calculated with propagation of error. $f(z,\Psi)$ denotes the denominator of Eq. (1), for which we adopted a relative error of 10% based on Wolff et al. (2010). For the uncertainty in NH_3 concentration measurements (δ_χ) we assumed the value of 1.9% determined by Wichink Kruit et al. (2007). As we have four methods to calculate the flux (two times using the α-factor and two times using the HF07/08 method), we calculated the mean of the error of all methods. This gave a median random error of 0.043 μg m^{-3} or ~50% (1σ) on the NH_3 flux. The random error varies throughout the day and year (Fig. A.1) and can be up to ~65% around noon or ~175% in spring 2010. When aggregating (e.g., when calculating a yearly deposition load), the random error will reduce by a factor $\sqrt{N}$.

The second source of error is associated with the choice of the method we used to account for the RSL. As all methods worked well on average, we had no reasons to prefer one over the other. Hence we used the standard error (SE) of the fluxes derived using the four methods as uncertainty range due to the RSL. Fig. A.1 shows the median diurnal pattern of the uncertainty due to the different methods. This introduced a median error of 0.012 μg m^{-3} or ~15% (1σ) to the NH_3 flux and could be up to ~18% in the early morning or ~25% in Autumn 2010 (Fig. A.1c). Note that this is considered as a systematic error.

The third source of error is due to a possible systematic error in the GRAHAM concentration measurements at one or multiple heights. It was not possible to determine a systematic error in the field due to the complexity of the measurement setup in the tower. Therefore, we used the systematic error of 0.6% which was determined by Wichink Kruit et al. (2007) under lab conditions. An error of 0.6% translates in a worst-case-scenario to an error of ~40 % (2σ) in the flux.

Finally, the fourth source of error is due to the high number of gaps in the dataset. This error can only be quantified on an annual scale and is relevant for the estimation of the annual deposition load. In total, we had only 36.4% concentration measurements and 13.5% flux measurements and data cover is not uniform over the year and day. We gap-filled the flux data for the hours for which only concentration values were present with the DEPAC-1D model (see Section 2.5.1). We determined the error due to gap-filling by taking the standard deviation of the residual errors (for hours where we have both model output and observed fluxes), which led to an error of ~5% (1 σ). Next, we determined the error due to the remaining gaps. Following Vendel et al. (2023), we quantified the imposed uncertainty by creating artificial gaps, of similar relative size as the actual gaps, on the measurements series of NH_3-fluxes without gaps. We repeated this exercise 1000 times and the standard deviation of the mean fluxes gives a random uncertainty of ~15% (1σ). Together this results in an error of ~18% (1 σ).

For an uncertainty estimate of the annual deposition load, the random error is not relevant as it becomes very small due to a reduction by factor $\sqrt{N}$. The other three errors, however, remain relevant. A total estimate of the flux error was achieved by quadratic summation of the individual errors. This gave a total uncertainty of ~30% (1σ) on yearly aggregated fluxes.

2.5. DEPAC-1D

2.5.1. Model description

DEPAC (DEposition of Acidifying Components) uses the resistance analogy to calculate fluxes from single level concentrations of various compounds and for NH_3 it also includes canopy compensation points (van Zanten et al., 2010; Wichink Kruit et al., 2010). DEPAC is a module within atmospheric chemistry transport and dispersion and deposition models such as LOTOS-EUROS (Manders et al., 2017) and OPS (Sauter et al., 2023), which are used in the Netherlands to assess and forecast air pollution and N-deposition but can also be used as a standalone inferential model. In this study, we used DEPAC as described in van Zanten et al. (2010).

The total resistance (or conductance) is calculated as the sum of the reciprocal aerodynamic resistance (r_a), the boundary layer resistance (r_b) and the canopy resistance (r_c). DEPAC calculates r_c as the sum of the reciprocal stomatal resistance (r_s), external leaf water resistance (r_w) and effective soil resistance ($r_{soil,eff}$):

$$1/r_c = 1/r_s + 1/r_w + 1/r_{soil,eff}, \tag{8}$$

while r_a and r_b are calculated in a shell around DEPAC. The exchange velocity can subsequently be calculated with:

$$v_e = 1/r_a + 1/r_b + 1/r_c \tag{9}$$

DEPAC uses, in addition to the resistance analogy, a compensation point for the r_s (χ_s) and r_w (χ_w) pathways. A compensation point for the soil pathway exists (χ_{soil}), but is currently set to zero in DEPAC. The separate compensation points are calculated using their respective emission potential (Γ_s and Γ_w). The total compensation point can be calculated as:

$$\chi_{tot} = \left[\frac{r_c}{r_w}\cdot\chi_w + \frac{r_c}{r_{soil,eff}}\cdot\chi_{soil} + \frac{r_c}{r_s}\cdot\chi_s\right]. \tag{10}$$

Finally, the flux magnitude and direction is determined with:

$$F_{NH_3} = -v_e\cdot(\chi_a - \chi_{tot}) \tag{11}$$

2.5.2. Stomatal compensation point

The emission potential of the stomatal pathway Γ_s is estimated with the following relation (Wichink Kruit et al., 2010):

$$\Gamma_s = 362\cdot\chi_a \tag{12}$$

where χ_a is calculated as the average $[NH_3]$ during the previous month. The number 362 is an empirically derived constant (Wichink Kruit et al., 2010).

The stomatal compensation point (χ_s) can be estimated from atmospheric observations by filtering for conditions when the external leaf exchange and the soil exchange are negligible compared to the stomatal exchange. During daytime ($R_{s,in} > 10$), turbulent ($\zeta < 0.1$) and dry conditions ($RH < 60\%$ and dry leaf wetness sensors) the stomatal exchange is much larger than the external leaf exchange ($F_{stom} \gg F_w$). Furthermore, we assumed the effective soil exchange to be close to zero due to the tall canopy and high LAI. Finally, when the NH_3 flux is near zero ($|F_{NH_3}| < 0.02$ μg m^{-2} s^{-1}) the atmospheric $[NH_3]$ resembles the stomatal compensation point (i.e. $\chi_a \approx \chi_s$).

According to Henry's law, χ_s should be in equilibrium with the dissolved $[NH_4^+]$ in the apoplastic fluid. This is also referred to as the emission potential (Γ_s) and is a commonly used parameter in models to account for compensation points (e.g. van Zanten et al., 2010; Massad et al., 2010). Γ_s can be calculated following Nemitz et al. (2001) and Wichink Kruit et al. (2007) with:

$$\chi_s = \frac{2.75\cdot10^{25}}{T_s}\exp\left(\frac{-1.044\cdot10^4}{T_s}\right)\cdot\Gamma_s \tag{13}$$

where T_s denotes the leaf surface temperature in Kelvin and Γ_s the dimensionless apoplastic $[NH_4^+]/[H^+]$ molar ratio. Surface temperature T_s can be approximated with $R_{l,out}$ using the Stefan–Boltzmann law and rewriting Eq. (13) allows to determine Γ_s.

2.5.3. Reference run

The DEPAC reference run is fed with observations of $[NH_3]_{44}$ from the 44 m level, local turbulence (as measured by the sonic anemometer) and local meteorology measured by the top level sensors. Furthermore, we use site dependent variables such as the roughness length (z_0 = 1.3 m (Weligepolage et al., 2012)), h_c (= 32 m) (Su et al., 2009) and LAI (= 6.1 m^{2}m^{-2}) Mustafa et al. (2013), which we assumed to stay constant during the measurement period. To account for co-deposition with SO_2 we used SO_2 concentration measurements at a nearby station in Eibergen, approximately 65 km east of the observation tower (taken from https://data.rivm.nl/data/luchtmeetnet/). As in the Netherlands SO_2 concentrations are generally low, we considered this spatial separation a negligible source of uncertainty. DEPAC calculates hourly averaged fluxes and for consistency in the comparison of model output and observations we average the observed fluxes to hourly fluxes.

3. Results

3.1. Timeseries of the 2009–2010 measurement period

Fig. 2a, b and c show the NH_3 concentration at 44 m, measured flux and cumulative flux throughout the measurement period. In both years, there was a peak in $[NH_3]$ in early spring (March/April) and in midsummer (July/August). However, the annual median pattern in 2010 shows much more variability than in 2009 (with both a higher maximum and a lower minimum). Throughout the entire measurement period, the $[NH_3]$ varied between 0.2 and 62.8 μg m^{-3}, with a mean of 6.0 μg m^{-3} and a median of 4.8 μg m^{-3} (N = 12 771). The (cumulative) flux time series showed three major deposition events: In April-May 2009, October-November 2009, and in October-November 2010. Emission events were observed during the entire measurement period, with especially strong events in July/August 2009 and May/June 2010. Throughout the entire measurement period the flux varied between −1.9 and 1.4 μg m^{-2} s^{-1} with a mean of −0.050 μg m^{-2} s^{-1} and a median of −0.036 μg m^{-2} s^{-1} (N = 4715).

The $[NH_3]$ patterns in Fig. 2a are similar for 2009 and 2010, with higher concentrations in early spring and summer and lower concentrations in late spring and autumn. The average $[NH_3]$ was higher in 2009 (6.4 μg m^{-3}) than in 2010 (5.4 μg m^{-3}). The deposition/emission patterns in Fig. 2c were roughly the same for overlapping periods in 2009 and 2010, i.e., with almost no net flux from July-September and deposition again in autumn. The most distinctive difference is in spring, where in 2009 strong deposition was measured, as opposed to emission in 2010. Interestingly, the cumulative flux in 2010 seems to be smaller than in 2009. This is both a result of a smaller data coverage and smaller deposition in spring 2009 compared to spring 2010.

Fig. 2c shows that cumulative the MOST and MOST-RSL flux calculations gave approximately the same result. The bandwidth denotes the standard error (SE) due to the four different MOST-RSL methods. Fig. A.2 shows the median diurnal cycles of the four separate methods, together with the median diurnal cycle of the average of the four different methods (MOST+RSL), and for completeness MOST is also shown. The different methods show a large spread, especially during nighttime, with some methods resulting in smaller fluxes and some in large fluxes compared to MOST. This resulted in the mean of the different MOST-RSL methods being similar to MOST.

3.2. Diurnal patterns

We divided the dataset into two sectors based on the median concentration: Northwest (NW) with low $[NH_3]$ and southeast (SE) with high $[NH_3]$ (see also Fig. 3). These sectors are also indicated in Fig. 1. Note that the southwest sector is smaller for fluxes than for concentrations (see also Table 1). Next, we divided the dataset into four seasons to investigate the effect of seasonality on the diurnal patterns.

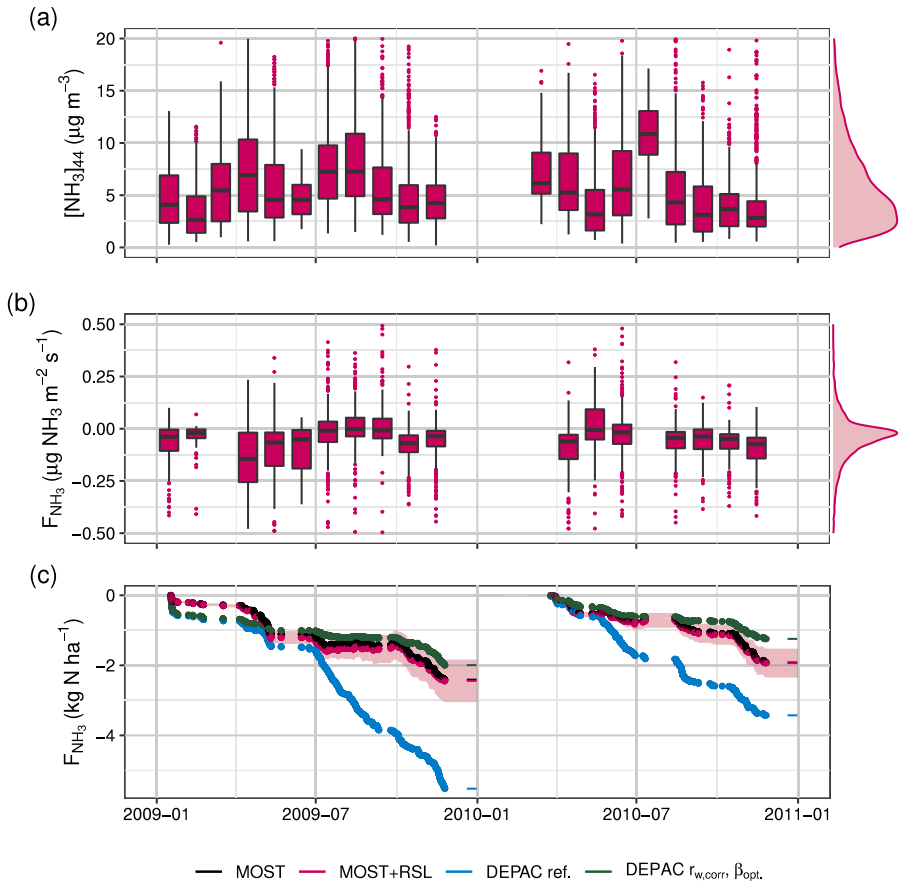

Fig. 2. Timeseries and histogram of (a) the NH_3 concentration at 44 m. The *y*-axis is cut-of at 20 µg m^{-3}, which excludes 185 meausurements. (b) Timeseries of the NH_3 flux with MOST+RSL. Note that the boxplots are not shown when N < 50. Furthermore, the *y*-axis is zoomed in to emphasize the main results. This results in an omission of in total 16 half hours with emission and 37 half hours with deposition. (c) Cumulative flux (only observations, no gap filling) is shown separately for the two years. The bandwidth indicates the error due to the different RSL methods. The cumulative fluxes for the DEPAC runs are also shown and will be further discussed in Section 3.3.3. At the end of the year the final value is indicated with a thin line.

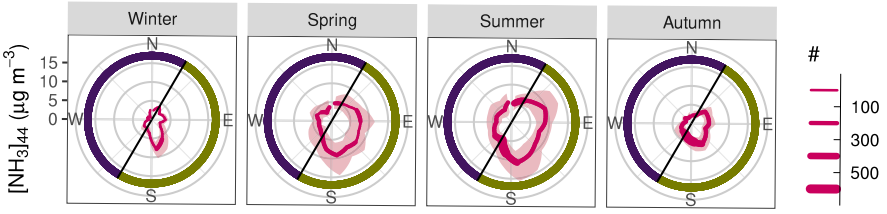

Fig. 3. Median $[NH_3]_{44}$ vs wind direction for each season. The bandwidth indicates the 25/75 percentile and the line width denotes the sample size (#). The two sectors are shown in dark purple (northwest, NW) and green (southeast, SE).

3.2.1. Concentrations

Fig. 4 shows the median diurnal cycles for the $[NH_3]$ per season and sector. Note that in winter the number of measurements was limited and thus care has to be taken when interpreting the results. In general, the $[NH_3]$ was higher in the SE sector than in the NW sector, confirming the results of Fig. 3. Towards the south/southeast of the measurement tower there is some agricultural activity which is a source of NH_3 and can explain the higher values. $[NH_3]$ was higher in both sectors during spring and summer than during winter and autumn. This can be explained by the stronger agricultural activity (by manure application and subsequent NH_3 emissions) and higher temperatures (causing more evaporation of NH_3) during these periods.

The median $[NH_3]$ in the SE sector in the morning in spring showed alternating values between ~6 and ~8 µg m^{-3}. This is an artifact caused by the differences in concentration between spring in 2009 (higher $[NH_3]$) and spring 2010 (lower $[NH_3]$) and is not apparent in the mean (not shown here). In winter, spring and autumn, the shape of the diurnal patterns was similar for both sectors (with an offset), while in summer the patterns of the two sectors deviated more.

It is uncertain how representative our results are due to the low data coverage. Therefore, we can only speculate on the origin of specific features in the diurnal variability. During summer, the SE sector had high $[NH_3]$ during night and morning, while in the NW sector $[NH_3]$ had a minimum during night/early morning. This pattern may be linked to the nearby farms in south/southeast, where the $[NH_3]$ built up during the night and was transported towards the measurement tower. During the day, the boundary layer grew by entrainment and the $[NH_3]$ was diluted with less NH_3-rich air from the free troposphere. The minimum $[NH_3]$ in the NW sector correlates with lower temperatures but similar humidity conditions ($RH \approx 90\%$) compared to the SE sector. This may have resulted in stronger deposition upwind of the tower (due to the lower temperatures and humid air), causing a minimum in $[NH_3]$ during the early morning. A comparable minimum was also found in the $[NH_3]$ at the same moment in spring.

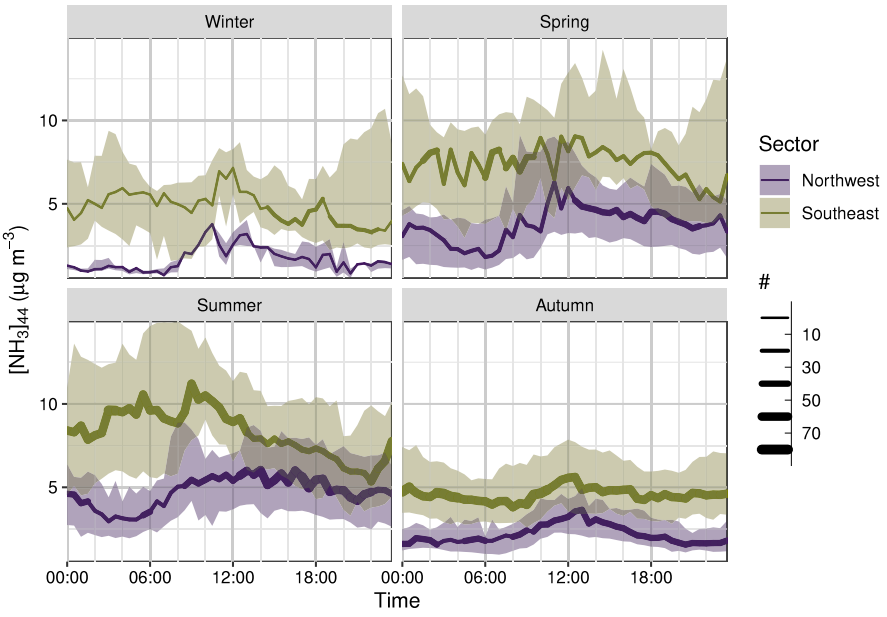

Fig. 4. Median diurnal patterns of [NH_3], grouped by sector and season. The shaded area indicates the 25/75 percentiles. The line width indicates the number of available measurements (#).

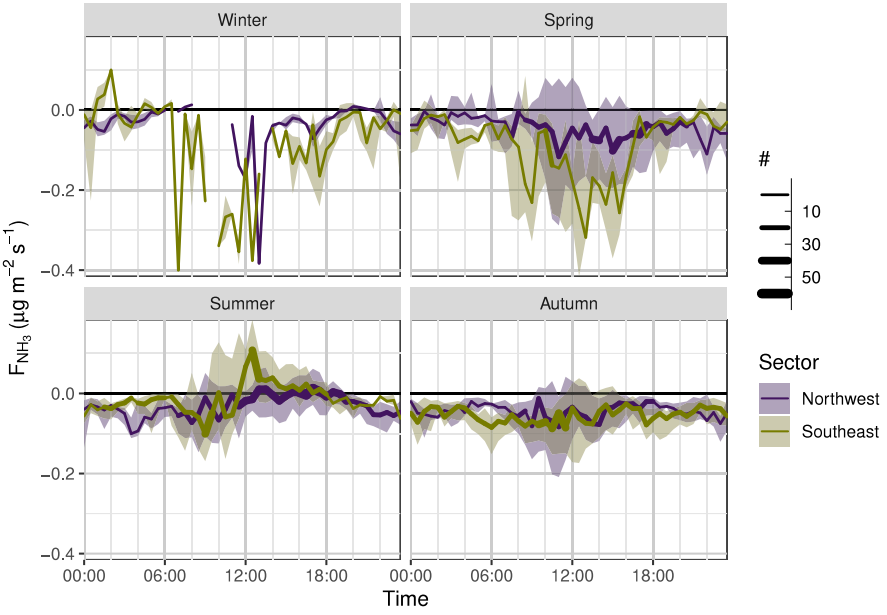

Fig. 5. Median diurnal patterns of F_{NH_3}, grouped by sector and season. The shaded area indicates the 25/75 percentiles. The line width indicates the number of available measurements (#).

3.2.2. *Fluxes*

Fig. 5 shows the median diurnal cycles for the NH_3 flux, grouped per season and sector. Note that in winter the number of observations was very limited (# = 0–3) and hence it will not be further discussed. It can be seen that, mainly for the SE sector, there was a pronounced diurnal variability in spring and summer, but not in autumn. Spring was characterized by deposition, especially in the SE sector during daytime. In summer, especially in the SE sector, emissions were observed around noon. Autumn was characterized by deposition during the entire day.

As with the diurnal cycles in [NH_3], we can only speculate on the origin of certain features. The emission fluxes during summer could be caused by the higher temperatures, leading to more evaporation of NH_3 out of the stomata. Interestingly, these emissions are not clearly distinguishable from the diurnal cycles in Fig. 4. This indicates that, from an NH_3 budget point of view, diurnal variability is also influenced by advection and/or entrainment. Schulte et al. (2021) showed that entrainment is especially important in the morning, but can also be relevant during the afternoon.

3.3. *DEPAC-1d*

3.3.1. *Reference run vs observations*

Fig. 2c shows the cumulative sum of the observed and DEPAC modelled fluxes and Fig. 6 shows their diurnal variations. The DEPAC reference run seems to overestimate the deposition, especially during summer and to a lesser extent during spring. However, the largest difference in the cumulative flux was due to the fact that the reference run did not predict any emissions. A large part of the diurnal cycle, however, was captured. This indicates that (most of) the exchange

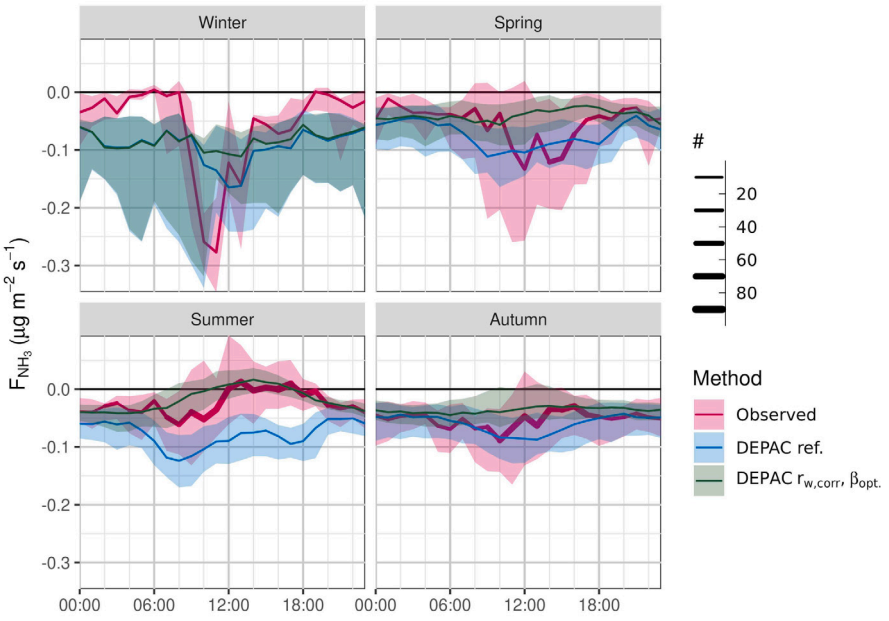

Fig. 6. Median diurnal patterns of F_{NH_3} for the observations, DEPAC reference run (see Section 2.5.3) and optimized DEPAC run for Speulderbos for each season. The bandwidth indicates the 25/75 percentiles and the line width of the observations show the number of measurements (#) for the respective time interval for both observations and the different DEPAC runs.

Table 2
Overview of statistics of observations and different DEPAC runs that passed filter criteria in Table 1. The mean and median fluxes are given in µg m^{-2}s^{-1}. RMSE shows the root mean squared error, MB the mean bias and NSE the Nash–Sutcliffe model efficiency. The values in brackets show the results for a subset where $r_w \ll r_s$ (see Section 3.3.3).

	Observed	DEPAC ref.	DEPAC $r_{w,corr}$	DEPAC $r_{w,corr}, \beta_{opt}$
Mean F_{NH_3}	−0.052 (−0.067)	−0.084 (−0.094)	−0.057 (−0.084)	−0.039 (−0.071)
Median F_{NH_3}	−0.037 (−0.047)	−0.068 (−0.082)	−0.046 (−0.073)	−0.033 (−0.060)
RMSE		0.14 (0.082)	0.13 (0.080)	0.13 (0.078)
MB		−0.054 (−0.027)	−0.011 (−0.017)	0.013 (−0.004)
NSE		−0.28 (−0.11)	0.01 (−0.04)	0.00 (0.01)

processes are appropriately described by the model. An interesting difference is the two deposition peaks in the morning and late afternoon in summer which are modelled in DEPAC, but not observed (and to a lesser extent also visible in spring).

Table 2 summarizes the statistics of both observations and DEPAC and their comparison. The DEPAC reference run overestimated the mean flux with a factor 1.6 and the median flux with almost a factor 2. Next to the RMSE, and mean bias (MB), we applied the Nash–Sutcliffe model efficiency (NSE, Nash and Sutcliffe, 1970) to validate how successful DEPAC was in predicting the flux variability. The NSE is calculated as:

$$\mathrm{NSE} = 1 - \frac{\Sigma\left(F_{\mathrm{NH_3,obs}} - F_{\mathrm{NH_3,DEPAC}}\right)^2}{\Sigma\left(F_{\mathrm{NH_3,obs}} - \overline{F_{\mathrm{NH_3,obs}}}\right)^2} \tag{14}$$

When NSE = 0, the model performance is as good as the mean of the observations, when NSE = 1 all the variance is explained by the model and when NSE < 0 the model performes worse than the mean of the observations. Table 2 shows that the NSE is negative, and thus that the DEPAC reference run performed worse in predicting the flux than the average of the observations.

3.3.2. Stomatal compensation point

Table 3 shows the derived emission potential (Γ_s) values for both years, together with their annual median [NH_3]. The results from literature analysis by Wichink Kruit et al. (2010) are also shown in Fig. 7, together with the derived Γ_s in this study (no. 22 and 23). Here, the long-term [NH_3] refers for most studies to mean or median [NH_3]

Table 3
Median annual [NH_3] for each year, together with the emission potential (Γ_s), its standard deviation (σ_{Γ_s}) and the sample size (N).

Year	Median [NH_3] (N) [µg m^{-3}]	Γ_s (N) [–]	σ_{Γ_s} [–]
2009	5.3 (7304)	$1.5{\cdot}10^3$ (61)	$0.5{\cdot}10^3$
2010	4.2 (5467)	$1.7{\cdot}10^3$ (83)	$0.9{\cdot}10^3$

of the entire measurement period, which ranges from several weeks to a year. The results agree well with the previous studies, and a linear fit shows similar results as Eq. (12).

3.3.3. Optimization

Within the DEPAC module, the different exchange paths are parameterized with the resistance analogy. The r_w path is currently parameterized, based on laboratory measurements (Sutton and Fowler, 1993), as:

$$r_w = r_{w,min} \cdot \exp\left(\frac{100 - RH}{\beta_{r_w}}\right) \tag{15}$$

where $r_{w,min}$ is the minimum external leaf resistance (s m^{-1}), which is in DEPAC set to 2. RH denotes the relative humidity (%) and β_{r_w} is a vegetation dependent empirical factor which is set to 12 in DEPAC. $r_{w,min}$ was found to be different for several studies sites, related to the chemical background conditions. In areas with a higher a [SO_2], $r_{w,min}$ was shown to be lower (Sutton and Fowler, 1993), which is in accordance with the NH_3-SO_2 co-deposition theory (e.g. Erisman and

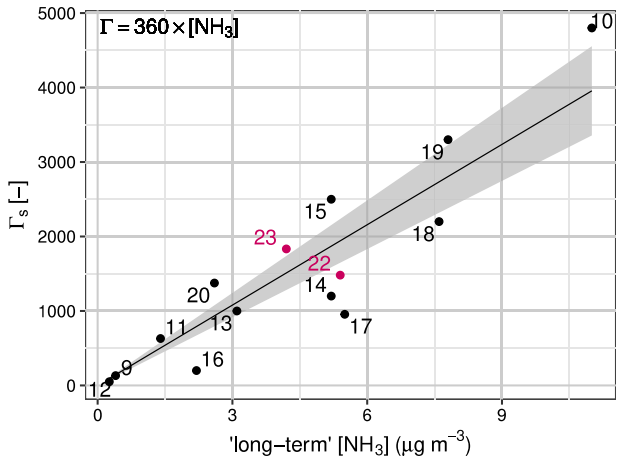

Fig. 7. Γ_s versus the 'long-term' [NH_3]. The black dots are reported values in literature and are all calculated with the micrometeorological method. The numbers correspond to the literature references in Table 5 from Wichink Kruit et al. (2010). The red dots with numbers 22 and 23 are the results of this study for 2009 and 2010 respectively (see also Table 3). The black line shows a linear fit with fixed intercept $y = 0$.

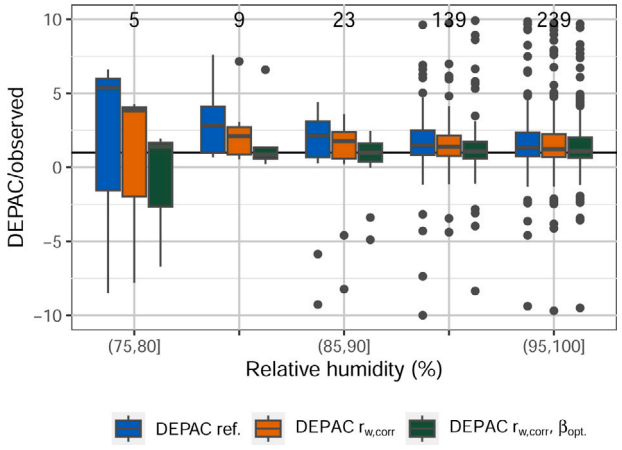

Fig. 8. Comparison of different DEPAC runs, as a function of the binned relative humidity (RH, %). The blackline shows y = 1 (where DEPAC = Observations) and the numbers at the top indicate the sample size of their respective bins.

Wyers, 1993). Flechard et al. (2010) showed r_w to be also dependent on surface temperature, in accordance with Henry's law (see also Eq. (13)). Furthermore, Zhang et al. (2003) suggests r_w to be also dependent on the LAI, as a larger surface area decreases the r_w. The two effects were combined in Eq. (15) by Massad et al. (2010) to:

$$r_{w,corr} = \frac{r_w \cdot \exp(0.15 \cdot T_s)}{SAI^{0.5}} \quad (16)$$

Here, we replaced the LAI by the surface area index (SAI, approximated with $SAI = LAI + 0.5$), which is a more appropriate variable for forests. T_s is the surface temperature (K), which we approximated by applying Stefan–Boltzmann's law to the measured long-wave outgoing radiation.

To test the new form of r_w, we filtered for conditions during which the external leaf pathway is dominant ($r_s \gg r_w$, i.e. night time, RH > 60% and leaf wetness sensors indicating wet leaves) and compared DEPAC and the observations during these conditions. Fig. 8 shows a comparison between DEPAC and observations against binned RH for the different DEPAC runs. The DEPAC reference run shows a clear overestimation of the flux at the lower RH range (75%–85%) but gets closer to the observations towards higher RH range. After implementation of Eq. (16) the results improve but a similar trend is still (although diminished) visible. Therefore, we adjusted the RH response of DEPAC by optimizing β_{r_w}. The results are shown for $\beta_{r_w} = 7$ in Fig. 8 and Table 2 (both for the entire dataset and for the subset as defined above). By lowering β_{r_w} from 12 to 7, the trend in RH response decreases further, but there is still some trend visible at the lower end (note that the number of observations here is limited). Further decreasing β_{r_w} affects the measurements in the higher RH range too much and the model performance gets worse. An overview of previous reported values for β_{r_w} is given in Table 1 of Massad et al. (2010). For coniferous forest, estimates for β_{r_w} ranges between 20 and 100. Considering all vegetation types, the lowest value reported for β_{r_w} is 2.6 (oilseed rape) and the maximum value is 125 (grassland). Although the optimized value is within the range of literature estimates, it is on the low side. Table 2 shows that the statistics on the r_w subset all improve compared to $\beta = 12$, but when comparing the performance on the entire dataset the results are similar to the reference run.

Fig. 6 shows the diurnal cycle after implementation of $r_{w,corr}$ and optimization of β_{r_w}. Especially the results in summer are improved, where DEPAC now also predicts emissions. This indicates that without the temperature correction on r_w, DEPAC predicts too much deposition. The final result is also plotted in Fig. 2c and it can be seen that the optimized version has a better agreement with observations than the reference run. The DEPAC performance has to a lesser extent also improved during spring and autumn, but some features in the observations are still missed, e.g., the deposition peak in spring mid-afternoon. To further investigate this, we subdivided the seasons into different years, see Fig. A.3. The fluxes in spring for the two years behave almost oppositely, where spring 2009 shows strong deposition fluxes during daytime and spring 2010 shows a minimum in deposition during daytime. DEPAC captures the diurnal cycle of 2010 well, but is not able to model the different behaviour of the diurnal cycle of 2009. This indicates that in spring 2009 a unknown process dominates the diurnal variation. A possible explanation could be that NH_4NO_3 gas-to-particle interconversion causes flux divergence, thereby violating one of the assumptions the AGM relies on. Previous studies have shown that this process can affect the NH_3 flux (Zhang et al., 1995; Nemitz, 2015; Katata et al., 2020), but that the effect is limited, especially in cases of large fluxes (Zhang et al., 1995). Unfortunately, we lack the observations to further investigate this. Finally, we adopted Eq. (16) from Massad et al. (2010) with quotient 0.15 and decided to optimize for β_w. However, our results indicate that the temperature correction is in certain cases (e.g., autumn 2010) too strong and the quotient of 0.15 may in fact also need optimization.

4. Discussion

4.1. RSL impact

From Section 3.1 and Figs. 2c and A.2 we saw that F_{NH_3} when calculated with MOST or with MOST+RSL are approximately equal. This is counter intuitive, as the RSL is characterized by enhanced turbulence compared to MOST and thus we would expect the cumulative flux for MOST+RSL to be larger than the cumulative flux for MOST. Based on the results of Melman et al. (2024a), we used four methods to incorporate the effects of the RSL in the flux calculation, and subsequently calculated their mean. Although all methods were on average able to reproduce H_{EC}, they deviate from each other on F_{NH_3}. Fig. A.2 shows that during winter and summer the methods agree well, but that especially in autumn the differences are large. Here, the $HF07/08_{obs}$ method deviates strongly from the other three methods.

We found no clear explanation for this deviating behaviour, but several things have to be considered. First, we applied the Harman and Finnigan (2008) RSL-modification on NH_3 instead of on the sensible heat flux. However, they found their framework to fail for carbon fluxes because they did not incorporate a source/sink distribution within the canopy. Although the source/sink distribution is not relevant above

the canopy as their influence should fade away towards the inertial sublayer (Harman and Finnigan, 2008), it has to be noted that our measurements, especially the bottom level, are very close to the canopy top. Hence, the local NH_3 sources and sinks within the canopy may influence their profile above the canopy more than would be predicted by the turbulent exchange coefficients alone. Furthermore, we assumed that the 'universal' ϕ-functions for heat and NH_3 are equal, which may not be the case due to the presence of other processes like chemical transformations (Vilà-Guerau de Arellano et al., 1995). To verify this assumption, simultaneous measurements with the AGM and EC have to be performed. Swart et al. (2023) undertook a study over grass that confirmed the comparability of the two methods. This indicates that the assumption of $\phi_H \approx \phi_{NH_3}$ may hold. Finally, we assume the displacement heights for NH_3, momentum and heat to be equal. All these assumptions have to be made due to a lack of alternatives and are valid from a turbulence point of view, but may not be valid for highly reactive scalars such as NH_3. This may have hampered to adequately describe NH_3 fluxes inside the RSL in any of the applied methods. Because the various RSL methods deal with these problems in a different way, we argue that using their ensemble to calculate the flux is an appropriate method to quantify the induced uncertainty.

Fig. A.2 shows that on average the differences between MOST and MOST+RSL are especially small during daytime, when the flux itself is also small. As our dataset is biased towards daytime, this contributes to the fact that MOST and MOST+RSL are very similar. At certain instances, however, the difference between MOST and MOST+RSL can be quite significant. In Fig. A.4 we plotted F_{NH_3} for 6 days in may 2010. During these days, the difference between MOST and MOST+RSL can be up to $\sim 30\%$. We expect that when data coverage is larger, e.g. with more nighttime fluxes or instances where daytime fluxes are large (see e.g. Fig. A.2), the differences will also be larger.

Furthermore, we want to stress the importance of applying an appropriate value for d. In Melman et al. (2024a), we optimized d by choosing the most appropriate method. When using the rule of thumb of $d = 2/3 \cdot h_c$ the flux would be strongly overestimated. Moreover, Harman and Finnigan (2007) argued that d should be considered as a function of the flow instead of as a constant. A constant d may in fact result in certain instances in an overestimation of the flux instead of the expected underestimation.

Finally, it must be noted that the exchange inside the RSL is physically different from exchange in the ISL, with an additional relevant length scale (i.e. the vorticity thickness) (Finnigan et al., 2009). Choosing an appropriate displacement height with MOST may give an on average correct flux, it is right for the wrong reasons. Hence, ignoring the enhanced turbulence may result in misinterpretations of the flux, especially within short campaigns. In the majority of the NH_3 exchange studies over forest, RSL enhanced turbulence is accounted for, but not in all. Although it may seem from our results that applying a RSL correction on MOST is not necessary, we strongly recommend to do so, in order to better describe the effects of the canopy on the turbulent fluxes.

4.2. Diurnal variability on seasonal scales

One of the main objectives was to identify diurnal cycles and asses their differences on a seasonal scale. In Section 3.2, we hypothesized on processes that could explain certain features in the diurnal patterns. To quantitatively explain the patterns the results would have to be combined with a Coupled Land Atmosphere model (e.g., Schulte et al., 2021) and an extensive study to the flux-drivers would have to be performed, which was beyond the scope of this study. Moreover, fluxes would have to be corrected for storage below the canopy, requiring $[NH_3]$ measurements below the canopy (e.g., Moncrieff et al., 2000), which were not present in this study.

In Section 3.2 and Figs. 4 and 5, we showed that there are distinct differences in $[NH_3]$ and F_{NH_3} between the different seasons (and sectors), with higher $[NH_3]$ in spring and summer, emissions in summer, and mostly deposition in spring and autumn. Only few studies have a measurement time-series that is suitable for analysis of seasonal patterns of NH_3 fluxes over forests. Xu et al. (2023) measured NH_3 fluxes in a (deciduous dominated) mixed forest in Japan for three periods of several weeks during different seasons and found similar patters for the different seasons as we did in this study. Neirynck and Ceulemans (2008) measured NH_3 fluxes in a deciduous forest in Belgium. They have divided their three-year dataset into periods with high daytime fluxes (February, May, June, July, August), and periods with daytime emission (April, August, September, November). This partly coincides with our results, where we only found strong daytime deposition in Spring (March, April, June) 2009. Wintjen et al. (2022) reports a two-year time-series of N_r fluxes in a remote mixed forest in Germany. They also found minor diurnal variations during autumn and emissions in spring (which we found only in 2010). Especially during summer, however, their results deviate from our findings, where they report mainly deposition while we observed also emissions. This difference may both be due to the fact that we are comparing NH_3 fluxes to N_r fluxes and due to the fact that their observation site is much more remote, with less pollution and thus a lower compensation point.

Finally, we saw that the patterns in the concentration cannot be solely explained by patterns in the surface flux (and/or the other way around). This indicates that other processes such as advection, entrainment, storage and chemical conversion also contribute to the NH_3 budget and can be strongly dominant over the surface exchange in their impact on the concentration (even when we filter for stationarity) (Schulte et al., 2021).

4.3. Estimation of annual deposition load

Unfortunately, our data coverage is too low to allow for year-round gap filling. Instead, we combined observed fluxes obtained with the AGM method with inferred fluxes obtained with the optimized form of DEPAC in order to derive the best representative annual deposition load. This is acceptable since we saw from Table 2 that the inferred fluxes based on the optimized form of DEPAC performed at least as well as the mean of the observed flux. Moreover, as can be seen in Fig. 2c the time series of the cumulative optimized DEPAC run is in strong agreement with observations, even though the diurnal cycle is in certain cases not well captured (see also Section 3.3.3). For the DEPAC inferred fluxes, we used the $[NH_3]_{44}$ that passed quality control according to Table 1 as input. Because DEPAC calculates hourly fluxes and our observed fluxes are in 30 min intervals, we averaged the observed fluxes to hourly values. This resulted in a total coverage of 43.3% for 2009 and 32.7% for 2010, of which 18.8 percentage point and 14.1 percentage point respectively were observed fluxes. With the assumption that the available dataset is representative for the entire year, we can extrapolate the median and mean fluxes to annual dry depositions loads. This gives 8.5 ± 2.6 (median) and 11.8 ± 3.5 (mean) kg N ha^{-1} for 2009 and 8.7 ± 2.6 (median) and 11.4 ± 3.4 (mean) kg N ha^{-1} for 2010, where the uncertainty range denotes 1σ and is calculated as the total uncertainty estimate of ~40% we found in Section 2.4.

It is likely that the annual deposition loads will be on the higher end of its uncertainty range: First, data cover is low, especially during winter months, and hence raises questions on its representativeness. To test the effect of a more evenly distributed coverage, we calculated the median and mean flux of each month per year and subsequently extrapolated these values to yearly deposition loads. With this, we would get a deposition load of 9.7 (median) and 14.6 (mean) kg N ha^{-1} in 2009 and 8.2 (median) and 11.7 (mean) kg N ha^{-1} in 2010. These numbers are, especially in 2010, comparable to the best estimates from the previous paragraphs and within (the higher end of) the uncertainty margin. Furthermore, the similarity between the estimates for 2009 and 2010 adds plausibility to their representativeness since they do not have an identical coverage (although the winter is underrepresented in

Table 4
Summary of the results of previous studies to NH_3 concentration and deposition at Speulderbos. # indicates the number of used measurements. Bold printed numbers are directly copied from the respective study. The yearly deposition loads are rounded to whole numbers.

Year	Concentration (μg m^{-3})			v_e (cm s^{-1})			Dry deposition (kg N ha^{-1} yr^{-1})				Reference
	Mean	Median	#	Mean	Median	#	Mean	Median	Estimate	#	
1988	10.0[c]	10.0[c]	11[c]	−5.0[c]	−6.9[c]	11	158[c]	148[c]	**50**[a]	11	Duyzer et al. (1992)
1989	3.8[c]	3.4[c]	24[c]	−4.2[c]	−3.9[c]	24	28[c]	36[c]	**50**[a]	24	Duyzer et al. (1992)
	4.4[b]				**−3.2**	1624		26[d]		1624	Wyers et al. (1992)
									21–44[a]		Duyzer et al. (1994)
1990	3.3[c]	3.1[c]	10	−2.8[c]	−5.1[c]	10	35[c]	44[c]	**50**[a]	10	Duyzer et al. (1992)
1993	5.6[b]						19[ba]				Wyers and Erisman (1998)
	5.8	**3.8**	4597								Vonk et al. (2000)
1994	4.5[b]						31[ba]				Wyers and Erisman (1998)
	4.7	**3.3**	4231								Vonk et al. (2000)
1995	**5.7**	**3.6**	4457	**−2.5**	**−2.5**	1603	**21**[a]	**11**[a]		4087	Vonk et al. (2000)
							21[ba]				Erisman et al. (2001a)
1997	**9.8**	**6.0**	3837	**−1.7**	**−1.3**	1344	**38**[a]	**14**[a]		2547	Vonk et al. (2000)
							22[ba]				Erisman et al. (2001a)
1998	**4.9**	**3.5**	2367	**−3.2**	**−2.6**	1109	**23**[a]	**15**[a]		2317	Vonk et al. (2000)
							26[ba]				Erisman et al. (2001a)
2009	6.4	5.3	7304	−1.4	−0.8	2719	12[a]	9[a]		7304[e]	This study
2010	4.8	3.2	5467	−1.5	−1.2	1996	11[a]	9[a]		5467[e]	This study

[a] Hybrid results based on observations and model results.
[b] Estimated from figure.
[c] Calculated from data in appendix.
[d] Calculated from median hourly flux.
[e] Total number of (30 min) observations, but averaged to hourly values.

both years). A more complete dataset will provide a better opportunity for advanced gap filling methods, e.g. by using machine learning (e.g. Zöll et al., 2019).

Second, from a physical point of view, we would expect that inside the RSL the exchange is enhanced compared to MOST and thus we expect the actual deposition load to be towards the end of the uncertainty estimate with an higher deposition load (see also Fig. 2).

4.4. Long term trends

Table 4 shows the NH_3 concentration and deposition measurements from previous studies performed at the Speulderbos. The measurements series started in 1988 but only few observations are available for that year and when calculating the mean or median flux from the 11 available hourly measurements the deposition load is unrealistically high. Instead, the authors provide an estimate of 50 kg N ha^{-1} yr^{-1} for the 1988–1990 period based on the average concentration reported by Vermetten et al. (1990) (5 μg m^{-3}) and the average parameterized exchange velocity (−3.6cm s^{-1}). Note that this model does not include a compensation point, while this is common in more recent models (e.g. Neirynck and Ceulemans, 2008) and thus the actual exchange velocity at the time may have been lower.

The follow-up studies have larger datasets and as such are more representative for the respective years. In 1997 both the concentration and deposition load reported by Vonk et al. (2000) are higher than the surrounding years. The authors state that this is mainly due to extremely high concentrations in March. When excluding this month the yearly deposition load is 30 kg N ha^{-1} instead. Unfortunately, we were not able to trace the large difference with the reported value of 22 kg N ha^{-1} by Erisman et al. (2001a) and just present the flux value as reported. For the remaining years, values reported by different studies are more comparable.

Interestingly, the annual deposition load differs strongly when using the mean or median flux with higher values for the median in 1988–1990 and lower values in 1995–1998. This indicates that the measurements within the respective datasets are highly variable and/or have a skewed distribution. For some years, different results have been reported by multiple studies, based on the same dataset. This is due to different data selection criteria or calculations, but may also be due to uncertainty arising from having to estimate the results from figures.

Fig. 9a shows the results of the historical datasets for [NH_3]; the mean [NH_3] of all LML stations are also added as a reference for [NH_3] changes over time. The LML [NH_3] timeseries are discussed in van Zanten et al. (2017), who found a decreasing trend up to 2004, after which the [NH_3] starts to increase again. From the historical measurements at the Speulderbos it seems that the [NH_3] has stayed approximately constant. Note that the LML timeseries is derived from nation-wide data, including measurement stations in NH_3 source areas, and is thus not directly representative for [NH_3] concentrations over nature areas. Moreover, LML stations measured year-round, while the historical datasets may be biased due to the low(er) coverage and hence miss e.g. months with higher concentrations.

Fig. 9b shows the annual estimates of F_{NH_3} of historical measurements, with the results of historical throughfall measurements (see Table A.1) added in black dots. Note that the latter are dry deposition estimates of NH_x which also include NH_4 aerosols, and thus shows a slightly different quantity (see also Erisman et al. (2001b) for a description of the methodology). Nevertheless, they provide an appropriate context to the dry deposition estimates from atmospheric measurements. It has to be noted that all measurements presented in this figure come with considerable uncertainties, barring us from drawing quantitative conclusions from them. Qualitatively, it can be stated that the [NH_3] has stayed approximately constant and that the annual deposition load has decreased between the early 1990's and 2010. The combined trends in [NH_3] and annual deposition load indicates that the deposition efficiency has decreased over the past decades (as can also bee seen from the exchange velocity in Table 4). This could be explained by the changing chemical climate, where in the Netherlands concentration of oxidized compounds such as SO_2 and NO_x has decreased. This has resulted in a less acidic surface and thus decreasing the NH_3 deposition potential (Wichink Kruit et al., 2017). A second explanation may lie in the changing character of the forest. The canopy height (h_c) has increased from 15 m in 1992 (Duyzer et al., 1992) to 32 m in 2006 (Su et al., 2009). Meanwhile, the LAI has decreased from estimates around 10 in 1991 to estimates ranging between 3.4 and 6.1 between 2006 and 2018 (Melman et al., 2024a). The strong decrease in LAI may be attributed to less trees in the forest (from 780–1000 ha^{-1} in 1989 to 375 ha^{-1} in 2006 Su et al., 2009), but

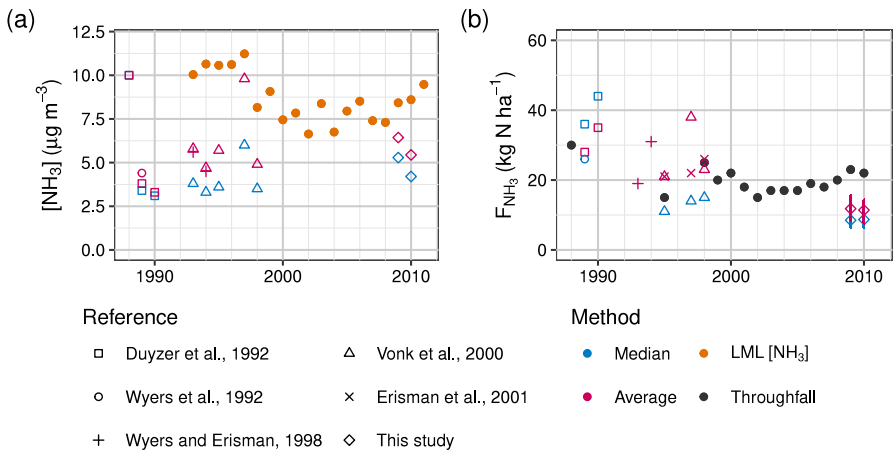

Fig. 9. (a) [NH_3] from historical dataset together with the national mean [NH_3] from the LML stations (van Zanten et al., 2017). (b) Annual deposition loads from historical datasets (from hybrid results based on observations and model results, see Table 4). The open points are atmospheric measurements of N-equivalents of NH_3 and the closed (black) points are estimates of N-equivalents of NH_x dry deposition from throughfall measurements.

might also be caused by changing methodologies over time to estimate the LAI. The two changes in the forest characteristics would have an opposite effect on forest roughness and hence on the F_{NH_3}. Overall, the changing chemical climate is likely to have the dominating effect, as this trend is also observed on a national scale (Wichink Kruit et al., 2017).

Finally, in Fig. 10 the total N_r deposition is estimated. The dry deposition of NH_3 was estimated by taking the average of each estimate within a single year of the values shown in Fig. 9. The wet deposition of both NH_x and NO_x was measured at Speulderveld, a field close to our measurement tower (<5 km) and part of the LML-network. Note that we do not have measurements of dry deposition of NO_y and NH_4 at Speulderbos and thus this had to be inferred with an alternate method. On a national scale, the contribution of dry deposition of NO_y is around 1.5 times the wet deposition of NO_y and the dry deposition of NH_4 is negligible (Hoogerbrugge et al., 2024). Therefore, we used the basic estimate of 1.5 $\cdot NO_{y,wet}$ for $NO_{y,dry}$, and ignored the contribution of $NH_{4,dry}$. Fig. 10 shows the resulting estimate of the total N_r deposition. The highest estimate for N_r deposition load is ~56 kg N ha^{-1} in 1994 and the lowest estimate is ~27 kg N ha^{-1}. The total N-stock in the soil of Dutch forests has increased with 1311 kg N ha^{-1} between 1990 and 2023, which would have required an average atmospheric N_r input of 50 kg N ha^{-1} yr^{-1} (de Jong et al., 2024). This estimate is higher than the estimates from Fig. 10, where in the early 1990's the total N-deposition was around 50 kg N ha^{-1} yr^{-1} and since 2000 it has been lower than this estimate. This difference might (partly) be caused by the fact that in our estimate the deposition of organic nitrogen is not taken into account (Sleutel et al., 2009; Ham and Tamiya, 2007).

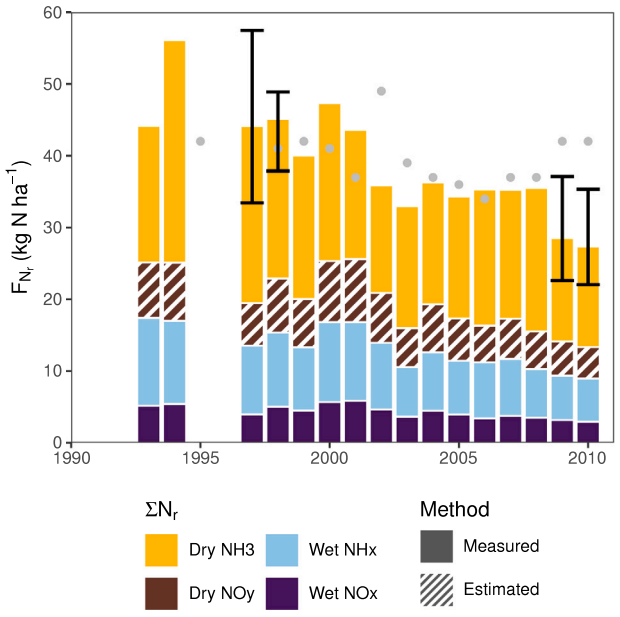

Fig. 10. Estimation of total N_r deposition. The yellow bars indicate the average of all dry NH_3 deposition measurements in each year as shown in Fig. 9 and the error bars represent their range. Dry deposition of NO_y is estimated based on wet deposition of NO_y (see main text for details). Years with missing estimates for dry NH_3 deposition or for wet deposition are omitted. For completeness, the total deposition estimates from throughfall measurements in Table 4 are also added and in grey dots.

4.5. Outlook

In this study we evaluated the NH_3 flux and concentration measurements, compared it to the DEPAC model and compared the most recent results with historically obtained data. It must be noted that what we presented as the 'observed' flux, is actually an inferred flux from a concentration gradient by making multiple assumptions; i.e. we used AGM. This also means that the observed and modelled fluxes are both based on the top level [NH_3] measurement, implying that they are not fully independent from each other, and as such the results and optimization of DEPAC have to be considered in that context. Recently, developments have been made with regard to fast analysers for NH_3, which can be used to apply the EC method (Wang et al., 2021; Swart et al., 2023; Guo et al., 2022). This technology will allow us to move from describing and monitoring fluxes to in-depth process studies. Moreover, it allows us to do a more proper and systematic comparison in which we can compare explicit observations of the NH_3 flux to inferred AGM and DEPAC parameterized fluxes.

In this study, we optimized DEPAC for a coniferous forest in the Netherlands, by implementing a temperature correction on the external leaf pathway and tuning one of the involved parameters. It is likely that the temperature correction is relevant for other forest, or even other vegetation types, as well, but that the tuned parameters have to be considered to be local. Further investigation into this has to reveal what the most representative value is. Finally, we fed the DEPAC reference run with local site characteristics, such as the z_0 and the LAI. It should be noted that models in which the DEPAC module is included, such as OPS and LOTOS-EUROS (see Section 2.5.1), use preset values for these site characteristics based on land-use class. So results of this study cannot be directly extrapolated to output from these models. Therefore, we recommend further research into how the

in this study proposed changes to DEPAC-1D behave in large scale atmospheric transfer models.

Finally, we compared our results to the historical results as they were presented at the time. Qualitatively, we found that dry deposition of NH_3 has decreased between 1990 and 2010, but were unable to quantify this trend due to the large uncertainties. Over the past decades, however, our knowledge on NH_3 exchange processes has strongly increased. A reanalysis of the historical data with up-to-date process knowledge may help to better quantify the trends during this period. Moreover, it allows for a unique possibility to investigate the ecosystem response to N_r input on decadal scale, and may reveal e.g. effects on carbon uptake. Meanwhile, since 2010 no new measurement campaign at the Speulderbos has been executed. A new measurement series would be a valuable addition to further investigate trends in N_r-deposition.

5. Conclusions

In this study, we analysed a two-year dataset of profile measurements of atmospheric ammonia concentrations ($[NH_3]$). $[NH_3]$ was measured with a GRAHAM (GRadient Ammonia High Accuracy Monitor) at three levels above a Douglas fir forest. We applied the aerodynamic gradient method to infer NH_3 fluxes (F_{NH_3}) and accounted for enhanced turbulence inside the roughness sublayer (RSL) with four different schemes. After quality control the total data coverage for $[NH_3]$ was 36.5% and for F_{NH_3} 13.5%. We subdivided the results into two wind direction sectors, northwest with low concentrations and southeast with high concentrations, and four seasons. Our main findings were:

- Including RSL turbulent conditions in the AGM calculations did on average not lead to enhanced fluxes. Based on a previous study (Melman et al., 2024a), we derived four different methods to account for the RSL and averaged the results of these separate methods (MOST+RSL). The results show a large spread, inducing an uncertainty band and on average similar results as would have been without correcting for the RSL (MOST). However, on certain instances the difference between MOST and MOST+RSL can be up to ~30%; indicating that accounting for enhanced turbulence in the RSL is important, especially with short measurement campaigns.
- We found a median $[NH_3]$ of 4.8 μg m^{-3} and a median F_{NH_3} of −0.036 μg m^{-2} s^{-1} and found both emission and deposition events. We identified four (potential) sources of error (i.e. random error, RSL error, error due to gaps and systematic error) and quadratic summation gave an average error of ~40% (1σ) on aggregated fluxes. Analysis showed that seasonal differences in diurnal variability are stronger than sectorial differences, both for concentrations and fluxes. We observed higher concentrations in spring and summer, mainly deposition in winter and autumn, and (strong) emission events in spring and summer. Annual patterns for 2009 and 2010 largely overlapped, but differences in spring were found, where in 2009 there was strong deposition while in 2010 we also observed emission of NH_3.
- We compared our observed fluxes with the 1D inferential model DEPAC. The emission potential (Γ_s) derived from atmospheric measurements agrees well with its parameterization in DEPAC. The reference run, however, overestimated the deposition and showed no emission fluxes. We were able to strongly improve the diurnal variability in DEPAC by implementing the leaf surface temperature as a driver for the external leaf resistance (r_w). This implementation also induced DEPAC to predict emission of NH_3. We were able to further improve the model performance by adjusting the r_w response to relative humidity (RH).
- We combined the observed fluxes with predicted fluxes by the optimized form of DEPAC to estimate the annual depositions loads. As data coverage was too low for meaningful gap-filling, we extrapolated the mean and median fluxes, which resulted in a deposition load of 11.8 ± 3.5 (mean) and 8.5 ± 2.6 (median) kg N $ha^{-1}yr^{-1}$ in 2009 and a deposition load of 11.4 ± 3.4 (mean) and 8.7 ± 2.6 (median) kg N $ha^{-1}yr^{-1}$ in 2010. We found that these numbers are probably representative for the entire year, but that the actual deposition is likely towards the higher end of the uncertainty estimate.
- At the Speulderbos atmospheric NH_3 concentration and exchange measurements had already been conducted in the early 1990's. Although the measurements have been carried out with a number of different measurement techniques, and come also with considerable uncertainties, it provided a unique opportunity to compare the results of this study to historically obtained datasets. The results indicated that the $[NH_3]$ has stayed approximately constant and that deposition decreased. This implies that the deposition process has become less efficient over the past decades, potentially due to a changing chemical climate, although the influence of changing forest characteristics cannot be ruled out.

CRediT authorship contribution statement

E.A. Melman: Writing – original draft, Visualization, Software, Methodology, Formal analysis, Conceptualization. **S. Rutledge-Jonker:** Writing – review & editing, Supervision, Conceptualization. **K.F.A. Frumau:** Methodology, Investigation. **A. Hensen:** Writing – review & editing, Investigation. **W.A.J. van Pul:** Writing – review & editing, Funding acquisition. **A.P. Stolk:** Investigation, Data curation. **R.J. Wichink Kruit:** Writing – review & editing, Software, Conceptualization. **M.C. van Zanten:** Writing – review & editing, Supervision, Software, Conceptualization.

Code and data availability

Data and code used to analyse flux and concentration data is available on https://doi.org/10.21945/17e65dbc-789d-44d7-b766-425475e30711(Melman et al., 2024b). Code used to calculate fluxes is available on request.

Declaration of competing interest

The authors declare that they have no known competing financial interests or personal relationships that could have appeared to influence the work reported in this paper.

Acknowledgements

The measurements were financed by the Dutch Ministry of Housing, Spatial Planning and the Environment. This study was supported by the Dutch Ministry of Agriculture, Nature and Food Quality (LNV), The Netherlands. The European Comission funded the NitroEurope IP and ITC provided a part of the instrumentation. The authors acknowledge the contributions of Jordi Vilà-Guerau de Arellano, Albert Bleeker and Jolien van Huijstee for providing the necessary background information.

Appendix

See Figs. A.1–A.4 and Table A.1.

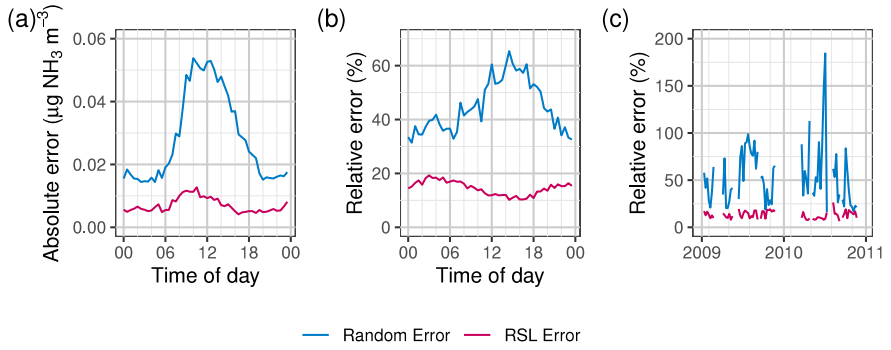

Fig. A.1. Mean diurnal variation of (a) absolute error and (b) relative error for (blue) random error and (red) error due to RSL. (c) Weekly average random error and error due to RSL.

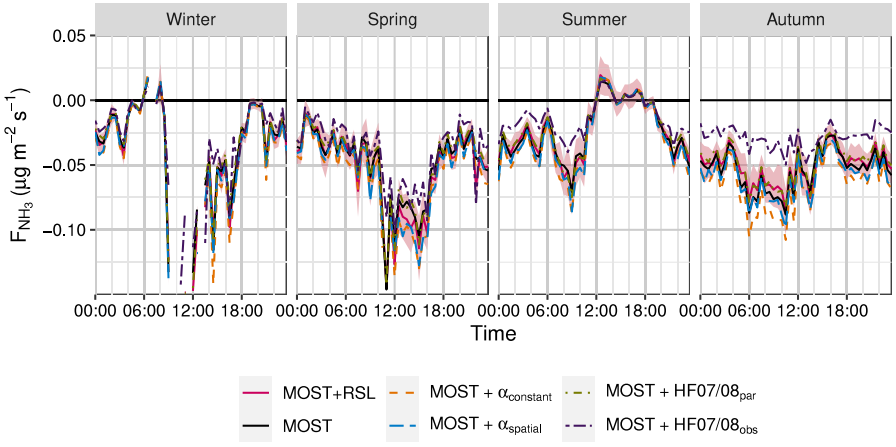

Fig. A.2. Median diurnal cycle for F_{NH_3} for each of the different methods separately and grouped by season. The solid-red line denotes the median diurnal cycle of the average of the four separate methods (MOST+RSL) and the shaded area denotes the standard error of the four separate methods. MOST without RSL corrections is denoted with a solid-black line. Note that the *y*-axis is cut-off at y = −0.15. This removes some data in winter.

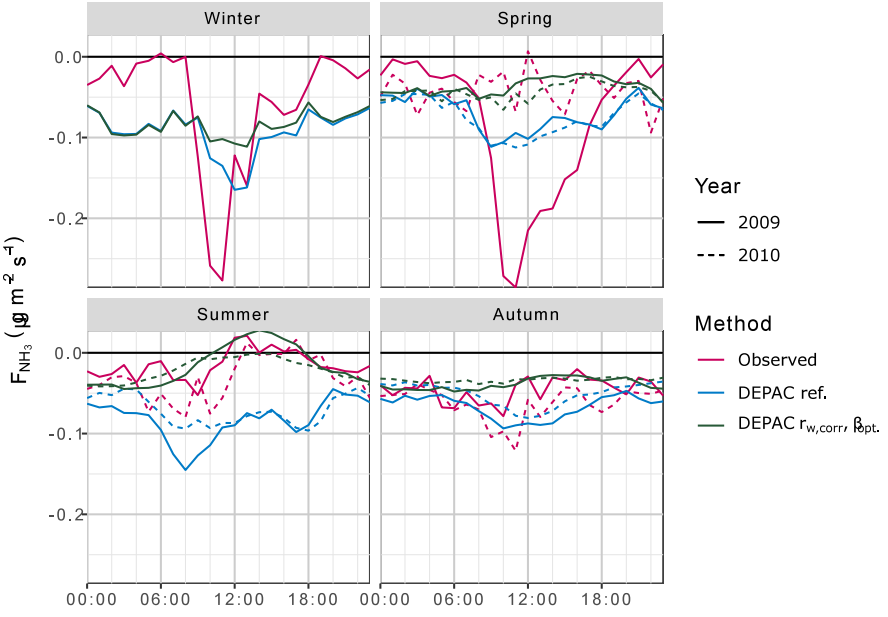

Fig. A.3. Mean diurnal variation for the observed and DEPAC modelled flux for each season and year.

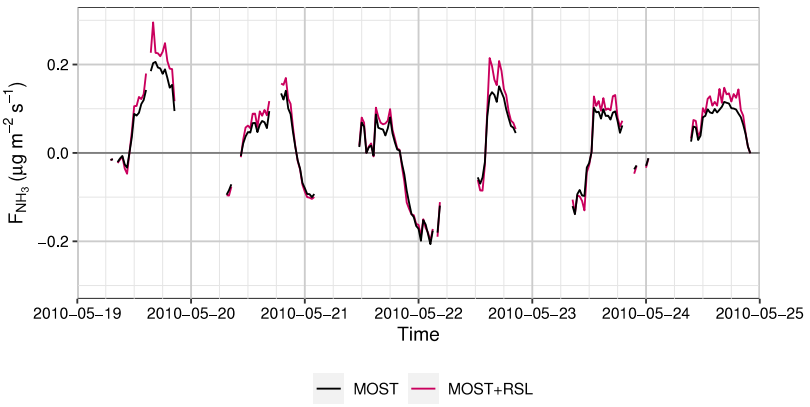

Fig. A.4. F_{NH_3} for 6 days in may 2010, calculated with both MOST and MOST+RSL.

Table A.1
Overview of throughfall measurements at Speulderbos of previous studies. The reported numbers are an estimate of the dry deposition of NH_x, which contains both NH_3 gas and NH_4^+ aerosols.

Year	Dry NH_x deposition kg N-NH_x ha^{-1} yr^{-1}	Total deposition kg N ha^{-1} yr^{-1}	Reference
1986	82		Draaijers et al. (1989)
1988	30		TNO Archives
1995	15[a]	42	Erisman et al. (2001b)
1998	25[a]	41	Erisman et al. (2001b)
1999	20[a]	42	Erisman et al. (2001b)
2000	22	41	Erisman et al. (2001b)
2001	21	37	Erisman et al. (2002)
2002	19	49	De Groot et al. (2003)
2003	17	39	Bleeker et al. (2004)
2004	17	37	Bleeker et al. (2005)
2005	17	36	Bleeker et al. (2008)
2006	19	34	TNO Archives
2007	18	37	TNO Archives
2008	20	37	TNO Archives
2009	23	42	Oldenburger et al. (2011)
2010	22	42	Oldenburger et al. (2011)

[a] Estimated from figure.

References

Andersen, H.V., Hovmand, M.F., Hummelshøj, P., Jensen, N.O., 1999. Measurements of ammonia concentrations, fluxes and dry deposition velocities to a spruce forest 1991–1995. Atmos. Environ. 33 (9), 1367–1383. http://dx.doi.org/10.1016/S1352-2310(98)00363-X.

Arya, S.P. (Ed.), 2001. Chapter 15 agricultural and forest micrometeorology. In: Introduction to Micrometeorology. In: International Geophysics, vol. 79, Academic Press, pp. 365–390. http://dx.doi.org/10.1016/S0074-6142(01)80031-0.

Beljaars, A.C.M., Holtslag, A.A.M., 1991. Flux parameterization over land surfaces for atmospheric models. J. Appl. Meteorol. Climatol. 30 (3), 327–341. http://dx.doi.org/10.1175/1520-0450(1991)030<0327:FPOLSF>2.0.CO;2.

Bleeker, A., De Groot, G., Möls, J., Fonteijn, P., Bakker, F., 2004. Throughfall Monitoring at 5 Sites in the Netherlands in 2003. Tech. Rep., ECN Petten, The Netherlands.

Bleeker, A., Geusebeek, M., van den Bulk, W., Fonteijn, P., 2005. Throughfall Monitoring at 5 Sites in the Netherlands in 2004. Tech. Rep., ECN Petten, The Netherlands.

Bleeker, A., Hicks, W., Dentener, F., Galloway, J., Erisman, J., 2011. N deposition as a threat to the world's protected areas under the convention on biological diversity. Environ. Pollut. 159 (10), 2280–2288. http://dx.doi.org/10.1016/j.envpol.2010.10.036.

Bleeker, A., van den Bulk, W., Fonteijn, P., Geusebroek, M., 2008. Deposition Monitoring at 5 Sites in The Netherlands in 2005. Tech. Rep., ECN Petten, The Netherlands.

Bosveld, F.C., 1997. Derivation of fluxes from profiles over a moderately homogeneous forest. Bound.-Layer Meteorol. 84, 289–327. http://dx.doi.org/10.1023/A:1000453629876.

Clark, C.M., Morefield, P.E., Gilliam, F.S., Pardo, L.H., 2013. Estimated losses of plant biodiversity in the United States from historical N deposition (1985–2010). Ecology 94 (7), 1441–1448. http://dx.doi.org/10.1890/12-2016.1.

De Groot, G., Erisman, J., Fossils, E.-C., Vermeulen, A., van der Klein, C., 2003. Throughfall Monitoring at 4 Sites in The Netherlands for 2002. Tech. Rep., ECN Petten, The Netherlands.

de Jong, J., de Vries, W., Dijk, P., Lerink, B., 2024. Veranderingen van voorraden koolstof, stikstof, fosfor, kalium, calcium, magnesium, ijzer en aluminium in bosbodems tussen 1990 en 2023. In: Rapport / Wageningen Environmental Research, no. 3362, Wageningen Environmental Research, Netherlands, http://dx.doi.org/10.18174/669938.

De Ridder, K., 2010. Bulk transfer relations for the roughness sublayer. Bound.-Layer Meteorol. 134, 257–267. http://dx.doi.org/10.1007/s10546-009-9450-y.

de Vries, W., Schulte-Uebbing, L., Kros, H., Voogd, J.C., Louwagie, G., 2021. Spatially explicit boundaries for agricultural nitrogen inputs in the European union to meet air and water quality targets. Sci. Total Environ. 786, 147283. http://dx.doi.org/10.1016/j.scitotenv.2021.147283.

Draaijers, G., Ivens, W., Bos, M., Bleuten, W., 1989. The contribution of ammonia emissions from agriculture to the deposition of acidifying and eutrophying compounds onto forests. Environ. Pollut. 60 (1), 55–66. http://dx.doi.org/10.1016/0269-7491(89)90220-0.

Duyzer, J.H., Verhagen, H.L.M., Weststrate, J.H., Bosveld, F.C., 1992. Measurement of the dry deposition flux of NH3 on to coniferous forest. Environ. Pollut. 75 (1), 3–13. http://dx.doi.org/10.1016/0269-7491(92)90050-k.

Duyzer, J.H., Verhagen, H.L.M., Weststrate, J.H., Bosveld, F.C., Vermetten, A.W.M., 1994. The dry deposition of ammonia onto a Douglas fir forest in the Netherlands. Atmos. Environ. 28 (7), 1241–1253. http://dx.doi.org/10.1016/1352-2310(94)90271-2.

Dyer, A., 1974. A review of flux-profile relationships. Bound.-Layer Meteorol. 7, 363–372. http://dx.doi.org/10.1007/BF00240838.

Elbers, J., 1998. Eddy Correlation System: User Manual Version 2.0. Wageningen: Alterra, the Netherlands.

Erisman, J., Fossils, E.-C., de Groot, G., van der Klein, C., 2002. Throughfall Monitoring at 4 Sites in the Netherlands Between 1995 and 2001. Tech. Rep., ECN, Petten, the Netherlands.

Erisman, J., Hensen, A., Fowler, D., Flechard, C., Grüner, A., Spindler, G., Duyzer, J., Weststrate, H., Römer, F., Vonk, A., et al., 2001a. Dry deposition monitoring in Europe. Water Air Soil Pollut. Focus 1, 17–27. http://dx.doi.org/10.1023/A:1013105727252.

Erisman, J., Mennen, M., Fowler, D., Flechard, C., Spindler, G., Grüner, A., Duyzer, J., Ruigrok, W., Wyers, G., 1998. Deposition monitoring in Europe. Environ. Monit. Assess. 53, 279–295. http://dx.doi.org/10.1023/A:1005818820053.

Erisman, J., Möls, J., Fonteijn, P., Bakker, F., 2001b. Throughfall Monitoring at 4 Sites in the Netherlands Between 1995 and 2000. ECN, Petten.

Erisman, J.W., Wyers, G., 1993. Continuous measurements of surface exchange of SO2 and NH3; implications for their possible interaction in the deposition process. Atmos. Environ. A 27 (13), 1937–1949. http://dx.doi.org/10.1016/0960-1686(93)90266-2.

Farquhar, G.D., Firth, P.M., Wetselaar, R., Weir, B., 1980. On the gaseous exchange of ammonia between leaves and the environment: Determination of the ammonia compensation point. Plant Physiol. 66 (4), 710–714. http://dx.doi.org/10.1104/pp.66.4.710.

Finnigan, J.J., Shaw, R.H., Patton, E.G., 2009. Turbulence structure above a vegetation canopy. J. Fluid Mech. 637, 387–424. http://dx.doi.org/10.1017/S0022112009990589.

Flechard, C.R., Massad, R.-S., Loubet, B., Personne, E., Simpson, D., Bash, J.O., Cooter, E.J., Nemitz, E., Sutton, M.A., 2013. Advances in understanding, models and parameterizations of biosphere-atmosphere ammonia exchange. Biogeosciences 10 (7), 5183–5225. http://dx.doi.org/10.5194/bg-10-5183-2013.

Flechard, C.R., Spirig, C., Neftel, A., Ammann, C., 2010. The annual ammonia budget of fertilised cut grassland – part 2: Seasonal variations and compensation point modeling. Biogeosciences 7 (2), 537–556. http://dx.doi.org/10.5194/bg-7-537-2010.

Foken, T., Göockede, M., Mauder, M., Mahrt, L., Amiro, B., Munger, J., 2006. Post-field data quality control. In: Handbook of Micrometeorology, Ser. Atmospheric and Oceanographic Sciences Library. vol. 29, Springer, pp. 181–208. http://dx.doi.org/10.1007/1-4020-2265-4_9.

Guo, X., Pan, D., Daly, R.W., Chen, X., Walker, J.T., Tao, L., McSpiritt, J., Zondlo, M.A., 2022. Spatial heterogeneity of ammonia fluxes in a deciduous forest and adjacent grassland. Agricult. Forest. Meterol. 326, 109128. http://dx.doi.org/10.1016/j.agrformet.2022.109128.

Ham, Y.-S., Tamiya, S., 2007. Contribution of dissolved organic nitrogen deposition to total dissolved nitrogen deposition under intensive agricultural activities. Water Air Soil Pollut. 178, 5–13. http://dx.doi.org/10.1007/s11270-006-9109-y.

Hansen, K., Pryor, S.C., Bøgh, E., Hornsby, K.E., Jensen, B., Sørensen, L.L., 2015. Background concentrations and fluxes of atmospheric ammonia over a deciduous forest. Agricult. Forest. Meterol. 214, 380–392. http://dx.doi.org/10.1016/j.agrformet.2015.09.004.

Hansen, K., Sørensen, L.L., Hertel, O., Geels, C., Skjøth, C.A., Jensen, B., Boegh, E., 2013. Ammonia emissions from deciduous forest after leaf fall. Biogeosciences 10 (7), 4577–4589. http://dx.doi.org/10.5194/bg-10-4577-2013.

Harman, I.N., 2012. The role of roughness sublayer dynamics within surface exchange schemes. Bound.-Layer Meteorol. 142, 1–20. http://dx.doi.org/10.1007/s10546-011-9651-z.

Harman, I.N., Finnigan, J.J., 2007. A simple unified theory for flow in the canopy and roughness sublayer. Bound.-Layer Meteorol. 123, 339–363. http://dx.doi.org/10.1007/s10546-006-9145-6.

Harman, I., Finnigan, J., 2008. Scalar concentration profiles in the canopy and roughness sublayer. Bound.-Layer Meteorol. 129, 323–351. http://dx.doi.org/10.1007/s10546-008-9328-4.

Hayashi, K., Matsuda, K., Takahashi, A., Nakaya, K., 2011. Atmosphere-forest exchange of ammoniacal nitrogen in a subalpine deciduous forest in central Japan during a summer week. Asian J. Atmos. Environ. 5 (2), 134–143. http://dx.doi.org/10.5572/ajae.2011.5.2.134.

Hoogerbrugge, R., Braam, M., Siteur, K., Jacobs, C., Hazelhorst, S., Stefess, G., van der Swaluw, E., Wichink Kruit, R., Wesseling, J., van Pul, A., 2024. Uncertainty in the determined nitrogen deposition in the Netherlands. Status report 2023. http://dx.doi.org/10.21945/RIVM-2022-0085.

Katata, G., Matsuda, K., Sorimachi, A., Kajino, M., Takagi, K., 2020. Effects of aerosol dynamics and gas–particle conversion on dry deposition of inorganic reactive nitrogen in a temperate forest. Atmos. Chem. Phys. 20 (8), 4933–4949. http://dx.doi.org/10.5194/acp-20-4933-2020.

Kljun, N., Calanca, P., Rotach, M.W., Schmid, H.P., 2015. A simple two-dimensional parameterisation for flux footprint prediction (FFP). Geosci. Model Dev. 8 (11), 3695–3713. http://dx.doi.org/10.5194/gmd-8-3695-2015.

Manders, A.M.M., Builtjes, P.J.H., Curier, L., Denier van der Gon, H.A.C., Hendriks, C., Jonkers, S., Kranenburg, R., Kuenen, J.J.P., Segers, A.J., Timmermans, R.M.A., Visschedijk, A.J.H., Wichink Kruit, R.J., van Pul, W.A.J., Sauter, F.J., van der Swaluw, E., Swart, D.P.J., Douros, J., Eskes, H., van Meijgaard, E., van Ulft, B., van Velthoven, P., Banzhaf, S., Mues, A.C., Stern, R., Fu, G., Lu, S., Heemink, A., van Velzen, N., Schaap, M., 2017. Curriculum vitae of the LOTOS–EUROS (v2.0) chemistry transport model. Geosci. Model Dev. 10 (11), 4145–4173. http://dx.doi.org/10.5194/gmd-10-4145-2017.

Massad, R.-S., Nemitz, E., Sutton, M.A., 2010. Review and parameterisation of bi-directional ammonia exchange between vegetation and the atmosphere. Atmos. Chem. Phys. 10 (21), 10359–10386. http://dx.doi.org/10.5194/acp-10-10359-2010.

Melman, E., Rutledge-Jonker, S., Braam, M., Frumau, K., Moene, A., Shapkalijevski, M., Vilà-Guerau de Arellano, J., van Zanten, M., 2024a. Increasing complexity in aerodynamic gradient flux calculations inside the roughness sublayer applied on a two-year dataset. Agricult. Forest. Meterol. 355, 110107. http://dx.doi.org/10.1016/j.agrformet.2024.110107.

Melman, E., Rutledge-Jonker, S., Frumau, A., Hensen, A., van Pul, A., Stolk, A., Wichink Kruit, R., van Zanten, M., 2024b. Data and code for "measurements and model results of a two-year dataset of ammonia exchange over a coniferous forest in the Netherlands". http://dx.doi.org/10.21945/17e65dbc-789d-44d7-b766-425475e30711.

Mennen, M., Uiterwijk, J., van Putten, E., van Hellemond, J., Wiese, C., Regts, T., Hogenkamp, J., Erisman, J., Bosveld, F., Wyers, G., Otjes, R., 1997. Dry deposition monitoring over the Speulder forest. Description of the equipment and evaluation of the measuring methods. http://hdl.handle.net/10029/261387.

Moncrieff, J.B., Jarvis, P.G., Valentini, R., 2000. Canopy fluxes. In: Sala, O.E., Jackson, R.B., Mooney, H.A., Howarth, R.W. (Eds.), Methods in Ecosystem Science. Springer New York, New York, NY, pp. 161–180. http://dx.doi.org/10.1007/978-1-4612-1224-9_12.

Mustafa, Y.T., Tolpekin, V.A., Stein, A., 2013. Improvement of spatio-temporal growth estimates in heterogeneous forests using Gaussian Bayesian networks. IEEE Trans. Geosci. Remote Sens. 52 (8), 4980–4991. http://dx.doi.org/10.1109/TGRS.2013.2286219.

Nash, J., Sutcliffe, J., 1970. River flow forecasting through conceptual models part I — A discussion of principles. J. Hydrol. 10 (3), 282–290. http://dx.doi.org/10.1016/0022-1694(70)90255-6.

Neirynck, J., Ceulemans, R., 2008. Bidirectional ammonia exchange above a mixed coniferous forest. Environ. Pollut. 154 (3), 424–438. http://dx.doi.org/10.1016/j.envpol.2007.11.030.

Neirynck, J., Kowalski, A.S., Carrara, A., Ceulemans, R., 2005. Driving forces for ammonia fluxes over mixed forest subjected to high deposition loads. Atmos. Environ. 39 (28), 5013–5024. http://dx.doi.org/10.1016/j.atmosenv.2005.05.027.

Nemitz, E., 2015. Surface/atmosphere exchange of atmospheric acids and aerosols, including the effect and model treatment of chemical interactions. In: Massad, R.-S., Loubet, B. (Eds.), Review and Integration of Biosphere-Atmosphere Modelling of Reactive Trace Gases and Volatile Aerosols. Springer Netherlands, Dordrecht, pp. 115–149. http://dx.doi.org/10.1007/978-94-017-7285-3_5.

Nemitz, E., Milford, C., Sutton, M.A., 2001. A two-layer canopy compensation point model for describing bi-directional biosphere-atmosphere exchange of ammonia. Q. J. R. Meteorol. Soc. 127 (573), 815–833. http://dx.doi.org/10.1002/qj.49712757306.

Oldenburger, J., van den Briel, J., Bleeker, A., Rietra, R., 2011. FutMon Activiteiten in Nederland in 2009 En 2010. Tech. Rep., Stichting Probos, https://edepot.wur.nl/215267.

Owen, S., Leaver, D., Bealey, W., Wilson, R., Reis, S., Sutton, M., 2011. A new database for time-series monitoring data: the NitroEurope approach. iForest - Biogeosci. Forestry (5), 226–232. http://dx.doi.org/10.3832/ifor0595-004.

Paulson, C.A., 1970. The mathematical representation of wind speed and temperature profiles in the unstable atmospheric surface layer. J. Appl. Meteorol. Climatol. 9 (6), 857–861. http://dx.doi.org/10.1175/1520-0450(1970)009<0857:TMROWS>2.0.CO;2.

Pryor, S.C., Barthelmie, R.J., Sørensen, L.L., Jensen, B., 2001. Ammonia concentrations and fluxes over a forest in the midwestern USA. Atmos. Environ. 35 (32), 5645–5656. http://dx.doi.org/10.1016/S1352-2310(01)00259-X.

Sauter, F., Sterk, M., van der Swaluw, E., Wichink Kruit, R., de Vries, W., van Pul, W., 2023. The OPS-Model. Description of OPS 5.1.1.0. RIVM, Bilthoven.

Schilperoort, B., Coenders-Gerrits, M., Jiménez Rodríguez, C., van der Tol, C., van de Wiel, B., Savenije, H., 2020. Decoupling of a douglas fir canopy: a look into the subcanopy with continuous vertical temperature profiles. Biogeosciences 17 (24), 6423–6439. http://dx.doi.org/10.5194/bg-17-6423-2020.

Schulte, R., van Zanten, M., Rutledge-Jonker, S., Swart, D., Wichink Kruit, R., Krol, M., van Pul, W., Vilà-Guerau de Arellano, J., 2021. Unraveling the diurnal atmospheric ammonia budget of a prototypical convective boundary layer. Atmos. Environ. 249, 118153. http://dx.doi.org/10.1016/j.atmosenv.2020.118153.

Sleutel, S., Vandenbruwane, J., De Schrijver, A., Wuyts, K., Moeskops, B., Verheyen, K., De Neve, S., 2009. Patterns of dissolved organic carbon and nitrogen fluxes in deciduous and coniferous forests under historic high nitrogen deposition. Biogeosciences 6 (12), 2743–2758. http://dx.doi.org/10.5194/bg-6-2743-2009.

Su, Z., Timmermans, W.J., van der Tol, C., Dost, R., Bianchi, R., Gómez, J.A., House, A., Hajnsek, I., Menenti, M., Magliulo, V., Esposito, M., Haarbrink, R., Bosveld, F., Rothe, R., Baltink, H.K., Vekerdy, Z., Sobrino, J.A., Timmermans, J., van Laake, P., Salama, S., van der Kwast, H., Claassen, E., Stolk, A., Jia, L., Moors, E., Hartogensis, O., Gillespie, A., 2009. EAGLE 2006 – multi-purpose, multi-angle and multi-sensor in-situ and airborne campaigns over grassland and forest. Hydrol. Earth Syst. Sci. 13 (6), 833–845. http://dx.doi.org/10.5194/hess-13-833-2009.

Sutton, M., Fowler, D., 1993. A model for inferring bi-directional fluxes of ammonia over plant canopies. In: Proceedings of the WMO Conference on the Measurement and Modelling of Atmospheric Composition Changes Including Pollutant Transport. WMO, Geneva, pp. 179–182.

Sutton, M.A., Pitcairn, C.E.R., Fowler, D., 1993. The exchange of ammonia between the atmosphere and plant communities. In: Advances in Ecological Research. vol. 24, Elsevier, pp. 301–393. http://dx.doi.org/10.1016/S0065-2504(08)60045-8.

Swart, D., Zhang, J., van der Graaf, S., Rutledge-Jonker, S., Hensen, A., Berkhout, S., Wintjen, P., van der Hoff, R., Haaima, M., Frumau, A., van den Bulk, P., Schulte, R., van Zanten, M., van Goethem, T., 2023. Field comparison of two novel open-path instruments that measure dry deposition and emission of ammonia using flux-gradient and eddy covariance methods. Atmos. Meas. Tech. 16 (2), 529–546. http://dx.doi.org/10.5194/amt-16-529-2023.

Thom, A.S., Stewart, J.B., Oliver, H.R., Gash, J.H.C., 1975. Comparison of aerodynamic and energy budget estimates of fluxes over a pine forest. Q. J. R. Meteorol. Soc. 101 (427), 93–105. http://dx.doi.org/10.1002/qj.49710142708.

van Elzakker, B., Buijsman, E., Wyers, G., Otjes, R., 1995. The measurement of ammonia in the national air quality monitoring network (LML): (1) instrumentation and network set-up. In: Heij, G., Erisman, J. (Eds.), Acid Rain Research: Do we have enough answers? In: Studies in Environmental Science, vol. 64, Elsevier, pp. 439–442. http://dx.doi.org/10.1016/S0166-1116(06)80313-4.

van Zanten, M., Sauter, F., Wichink Kruit, R., van Jaarsveld, J., van Pul, W., 2010. Description of the DEPAC module: Dry deposition modelling with DEPAC GCN2010. https://www.rivm.nl/bibliotheek/rapporten/680180001.pdf.

van Zanten, M., Wichink Kruit, R., Hoogerbrugge, R., Van der Swaluw, E., van Pul, W., 2017. Trends in ammonia measurements in the Netherlands over the period 1993–2014. Atmos. Environ. 148, 352–360. http://dx.doi.org/10.1016/j.atmosenv.2016.11.007.

Vendel, K., Wichink Kruit, R., Blom, M., van den Bulk, P., van Egmond, B., Frumau, A., Rutledge-Jonker, S., Hensen, A., van Zanten, M., 2023. Dry deposition of ammonia in a coastal dune area: Measurements and modeling. Atmos. Environ. 298, 119596. http://dx.doi.org/10.1016/j.atmosenv.2023.119596.

Vermetten, A.W.M., Hofschreuder, P., Versluis, A.H., Bij, E.S.v., van Tongeren, J., Molenaar, E., Houthuyzen, J.D., in't Veld, F., 1990. Air Pollution in Forest Canopies. Wageningen Agricultural University, Dept. of Air Pollution, R-424.

Vilà-Guerau de Arellano, J., Duynkerke, P.G., Zeller, K.F., 1995. Atmospheric surface layer similarity theory applied to chemically reactive species. J. Geophys. Res.: Atmos. 100 (D1), 1397–1408. http://dx.doi.org/10.1029/94JD02434.

Vonk, A., Jaarsveld, J.v., Bleeker, A., van Putten, E., 2000. Towards development of a deposition monitoring network for air pollution of Europe (LIFE II). http://hdl.handle.net/10029/257659.

Walker, J.T., Chen, X., Wu, Z., Schwede, D., Daly, R., Djurkovic, A., Oishi, A.C., Edgerton, E., Bash, J., Knoepp, J., Puchalski, M., Iiames, J., Miniat, C.F., 2023. Atmospheric deposition of reactive nitrogen to a deciduous forest in the southern Appalachian Mountains. Biogeosciences 20 (5), 971–995. http://dx.doi.org/10.5194/bg-20-971-2023.

Wang, K., Kang, P., LU, Y., Zheng, X., Liu, M., Lin, T.-J., Butterbach-Bahl, K., Wang, Y., 2021. An open-path ammonia analyzer for eddy covariance flux measurement. Agricult. Forest. Meterol. 308–309, 108570. http://dx.doi.org/10.1016/j.agrformet.2021.108570.

Weligepolage, K., Gieske, A.S.M., Su, Z., 2012. Surface roughness analysis of a conifer forest canopy with airborne and terrestrial laser scanning techniques. Int. J. Appl. Earth Observ. Geoinf. 14 (1), 192–203. http://dx.doi.org/10.1016/j.jag.2011.08.014.

Wichink Kruit, R., 2010. Surface-Atmosphere Exchange of Ammonia: Measurements and Modeling Over Non-Fertilized Grassland in the Netherlands. Wageningen University and Research, https://edepot.wur.nl/137586.

Wichink Kruit, R., Aben, J., de Vries, W., Sauter, F., van der Swaluw, E., van Zanten, M., van Pul, W., 2017. Modelling trends in ammonia in the Netherlands over the period 1990–2014. Atmos. Environ. 154, 20–30. http://dx.doi.org/10.1016/j.atmosenv.2017.01.031.

Wichink Kruit, R., Bleeker, A., Braam, M., van Goethem, T., Hoogerbrugge, R., Rutledge-Jonker, S., Stefess, G., Stolk, A., van der Swaluw, E., Voogt, M., et al., 2021. Op weg naar een optimale meetstrategie voor stikstof. http://dx.doi.org/10.21945/RIVM-2021-0118.

Wichink Kruit, R., Stolk, A., Volten, H., van Pul, W., 2009. Flux Measurements of Ammonia at the Micrometeorological Weather Station in Wageningen, The Netherlands. RIVM Letter Report 680150004, Rijksinstituut voor Volksgezondheid en Milieu RIVM, https://www.rivm.nl/bibliotheek/rapporten/680150004.pdf.

Wichink Kruit, R.R., van Pul, W., Otjes, R., Hofschreuder, P., Jacobs, A., Holtslag, A., 2007. Ammonia fluxes and derived canopy compensation points over non-fertilized agricultural grassland in The Netherlands using the new gradient ammonia—high accuracy—monitor (GRAHAM). Atmos. Environ. 41 (6), 1275–1287. http://dx.doi.org/10.1016/j.atmosenv.2006.09.039.

Wichink Kruit, R., van Pul, W., Sauter, F., van den Broek, M., Nemitz, E., Sutton, M., Krol, M., Holtslag, A., 2010. Modeling the surface–atmosphere exchange of ammonia. Atmos. Environ. 44 (7), 945–957. http://dx.doi.org/10.1016/j.atmosenv.2009.11.049.

Wintjen, P., Schrader, F., Schaap, M., Beudert, B., Brümmer, C., 2022. Forest–atmosphere exchange of reactive nitrogen in a remote region – part I: Measuring temporal dynamics. Biogeosciences 19 (2), 389–413. http://dx.doi.org/10.5194/bg-19-389-2022.

Wolff, V., Trebs, I., Ammann, C., Meixner, F.X., 2010. Aerodynamic gradient measurements of the NH_3-HNO_3-NH_4NO_3 triad using a wet chemical instrument: an analysis of precision requirements and flux errors. Atmos. Meas. Tech. 3 (1), 187–208. http://dx.doi.org/10.5194/amt-3-187-2010.

Wyers, G.P., Erisman, J.W., 1998. Ammonia exchange over coniferous forest. Atmos. Environ. 32 (3), 441–451. http://dx.doi.org/10.1016/S1352-2310(97)00275-6.

Wyers, G., Otjes, R., Slanina, J., 1993. A continuous-flow denuder for the measurement of ambient concentrations and surface-exchange fluxes of ammonia. Atmos. Environ. A 27 (13), 2085–2090. http://dx.doi.org/10.1016/0960-1686(93)90280-C.

Wyers, G.P., Vermeulen, A.T., Slanina, J., 1992. Measurement of dry deposition of ammonia on a forest. Environ. Pollut. 75 (1), 25–28. http://dx.doi.org/10.1016/0269-7491(92)90052-C.

Xu, M., Chanonmuang, P., Matsuda, K., 2023. Vertical profile and flux measurements of ammonia in a deciduous forest in Japan towards improvement of bi-directional exchange model. Atmos. Environ. 315, 120144. http://dx.doi.org/10.1016/j.atmosenv.2023.120144.

Zhang, L., Brook, J.R., Vet, R., 2003. A revised parameterization for gaseous dry deposition in air-quality models. Atmos. Chem. Phys. 3 (6), 2067–2082. http://dx.doi.org/10.5194/acp-3-2067-2003.

Zhang, Y., ten Brink, H., Slanina, S., Wyers, P., 1995. The influence of ammonium nitrate equilibrium on the measurement of exchange fluxes of ammonia and nitric acid. In: Heij, G., Erisman, J. (Eds.), Acid Rain Research: Do We Have Enough Answers?. In: Studies in Environmental Science, vol. 64, Elsevier, pp. 103–112. http://dx.doi.org/10.1016/S0166-1116(06)80277-3.

Zhang, L., Wright, L.P., Asman, W.A.H., 2010. Bi-directional air-surface exchange of atmospheric ammonia: A review of measurements and a development of a big-leaf model for applications in regional-scale air-quality models. J. Geophys. Res.: Atmos. 115 (D20), http://dx.doi.org/10.1029/2009JD013589.

Zöll, U., Lucas-Moffat, A.M., Wintjen, P., Schrader, F., Beudert, B., Brümmer, C., 2019. Is the biosphere-atmosphere exchange of total reactive nitrogen above forest driven by the same factors as carbon dioxide? An analysis using artificial neural networks. Atmos. Environ. 206, 108–118. http://dx.doi.org/10.1016/j.atmosenv.2019.02.042.